# Assessing the Vulnerability to Climate in Prince William Sound Watersheds (AK)
# National Fish and Wildlife Foundation Project 46010

**Steve Wondzell**
**Pacific Northwest Research Station**
**Corvallis, OR**

**Luca Adelfio**
**Chugach National Forest**
**Cordova, AK**

**Nate Mantua**
**National Marine Fisheries Service**
**Santa Cruz, CA**

**Gordon Reeves**
**Pacific Northwest Research Station**
**Corvallis, OR**

## Abstract

We examined the potential effects of warming winters resulting from climate change on Pacific Salmon in Prince William Sound, AK. Winter air temperatures in this area are projected to increase 3$^{o}$c. The corresponding increase in water temperature was not uniform across the study but varied widely depending on water features. About 15% of the watersheds will moderately to highly susceptible to these changes, which will affect the time of spawning, development of eggs, and the time of and size at emergence of salmon fry. Additionally, fish that spawn earliest are likely to be most affected. This work will aid policy makers and managers to better understand the potential impacts of climate in Prince William Sound and to develop appropriate policies, practices, such as managing for population diversity rather than numbers, and adaptation programs to meet the challenges of a changing climate.

## Introduction

Climate change poses a major challenge to Pacific salmon (*Oncorhynchus* spp.) and the policy makers and managers responsible for their persistence. Warmer summer temperatures will reduce the suitability of freshwater habitats (Crozier and Zabel 2006, Isaak et al. 2010), potentially reducing growth rates, increasing disease susceptibility, and altering interactions with competitors and predators. Increased winter temperatures in the NWFP area will result in more precipitation falling as rain rather than snow. Watersheds that historically developed a seasonal snowpack will experience a trend from snow to rain, resulting in more rapid runoff in winter and early spring when snow usually falls, and lower late-spring and early-summer flows owing to reduced snowmelt (Hamlet and Lettenmaier 2007, Tague and Grant 2009), coupled with substantial reductions in summer low flows. Chilcote et al. (2017) estimated that 8.5% of the

watersheds on the Chugach National Forest in south central Alaska were vulnerable to similar changes in their hydrographs.

Another, but not well recognized, consequence of warmer winters is an increase in water temperature and the subsequent effects on developing eggs and embryos and phenology (ie., timing of life-history events) of Pacific salmon in northern latitudes. The rate of development of eggs and the size of fish at emergence is related to water temperature. Egg development depends on the accumulation of degree days (Neuheimer and Taggart 2007). Even slight increases in temperature can accelerate rate of development and ultimately result in earlier time of emergence from the gravel (McCullough 1999). This can result in a mismatch with the availability of prey and other food resources and required habitats. It can also result in smaller individuals at emergence because metabolic costs decrease the efficiency of yolk use (Beacham and Murray 1990, Elliott and Hurley 1998); smaller fish are more susceptible to displacement at higher flows.

The climate in Prince William Sound is anticipated to warm by 3 °C during the next 50 years (Fresco and Floyd 2017). Importantly, the greatest warming is anticipated in winter, pushing monthly mean air temperatures above freezing year-round near sea level. The extent of change in water temperatures in given area is likely to vary widely depending on local features. Elevation, water sources, and presence of glaciers, lakes and wetlands all influence water temperature (Adelfio et al. 2019). Understanding the extent of potential changes in winter water temperatures is critical to understand the potential vulnerability of population of Pacific Salmon to climate change and the development of adaptation and mitigation programs. The goal of this study was to assess the potential effects of changes in winter temperatures on water temperatures in streams in Prince William Sound, AK, a major producer of salmon locally and globally (Chilcote et al. 2017).

**Study Area**

The location of the study area and watersheds where air and water temperature were measured are shown in Fig. 1. The region's subarctic maritime climate is characterized by cool temperatures, a small annual temperature range, and abundant precipitation (Bieniek et al. 2012). The surrounding terrain is mountainous and high-relief, rises of over 4,000 m above sea level in less than 20 km. Tidewater glaciers and large icefields are present on the mainland, particularly along the northern and western coastline where the mountains are highest.

The surficial geology is most commonly sedimentary or igneous bedrock from the Eocene and Paleocene or unconsolidated glacial deposits from the Holocene and Pleistocene (Wilson et al. 2008). Below 600 m elevation, mature stands of Sitka spruce (*Picea sitchensis*), Mountain hemlock (*Tsuga mertensiana*), and, on the eastern side of PWS, Western hemlock (*T. heterophylla*) are the primary late successional vegetation species (Cooper, 1942). *Sphagnum*- or *Carex*-dominated peatlands, collectively known as "muskegs," are also common and widespread in undisturbed, late successional piedmont areas. Active glacier outwash plains and other disturbed areas are often thickly vegetated with brush, particularly Sitka alder (*Alnus viridis*).

See Appendix A for further details.

**Projecting Thermal Sensitivity across Prince William Sound**

We established 15 monitoring locations at known salmon spawning sites in PWS during the summer of 2013 (Figure 1). The study watersheds range from the Gulf of Alaska coast on Montague and Hinchinbrook Islands, to large glaciated mainland watersheds draining into northern PWS. The watersheds were distributed from east-to-west, across the PWS climate gradient.

We collected hourly air temperature and surface (stream) and shallow streambed water temperature data from 1 October, 2013 until 1 October, 2017. We recorded air temperature with a HOBO Pendant data logger housed in a gill radiation shield produced by the Onset Computer Corporation. We recorded surface water temperature at the bottom of the water column with 1 HOBO Pro v2 data logger housed in a 15-cm-long section of 4.1-cm internal diameter galvanized steel pipe to shade the sensor and protect it from physical damage. \We measured streambed water temperature 35 to 50 cm into the streambed using a TidbiT v2 data logger installed directly into the substrate after boring a hole with a custom-made driver (Zimmerman and Finn 2012). We deployed two streambed loggers at each site.

We downloaded data loggers every 6 to 12 months throughout the study period. We removed erroneous values, including unreasonable outliers (which suggest sensor error) and abnormally high hourly variance (>3°C), suggesting the sensor was exposed to air. Occasional data gaps occurred when streambed data loggers were exposed to surface water, surface water loggers were exposed to air, and when data loggers were lost, malfunctioned, or were not downloaded in 2018. The most prolific data gaps were for air temperature. Cold winter air temperatures reduced battery longevity, resulting in data logger failure in many cases.

Statistical relations between air and water temperatures and watershed features were then used to determine the potential sensitivity of watershed to changes in future temperatures and the impacts on developing eggs and embryos of Pacific salmon.

See Appendix A for details on temperature sensitivity analysis.

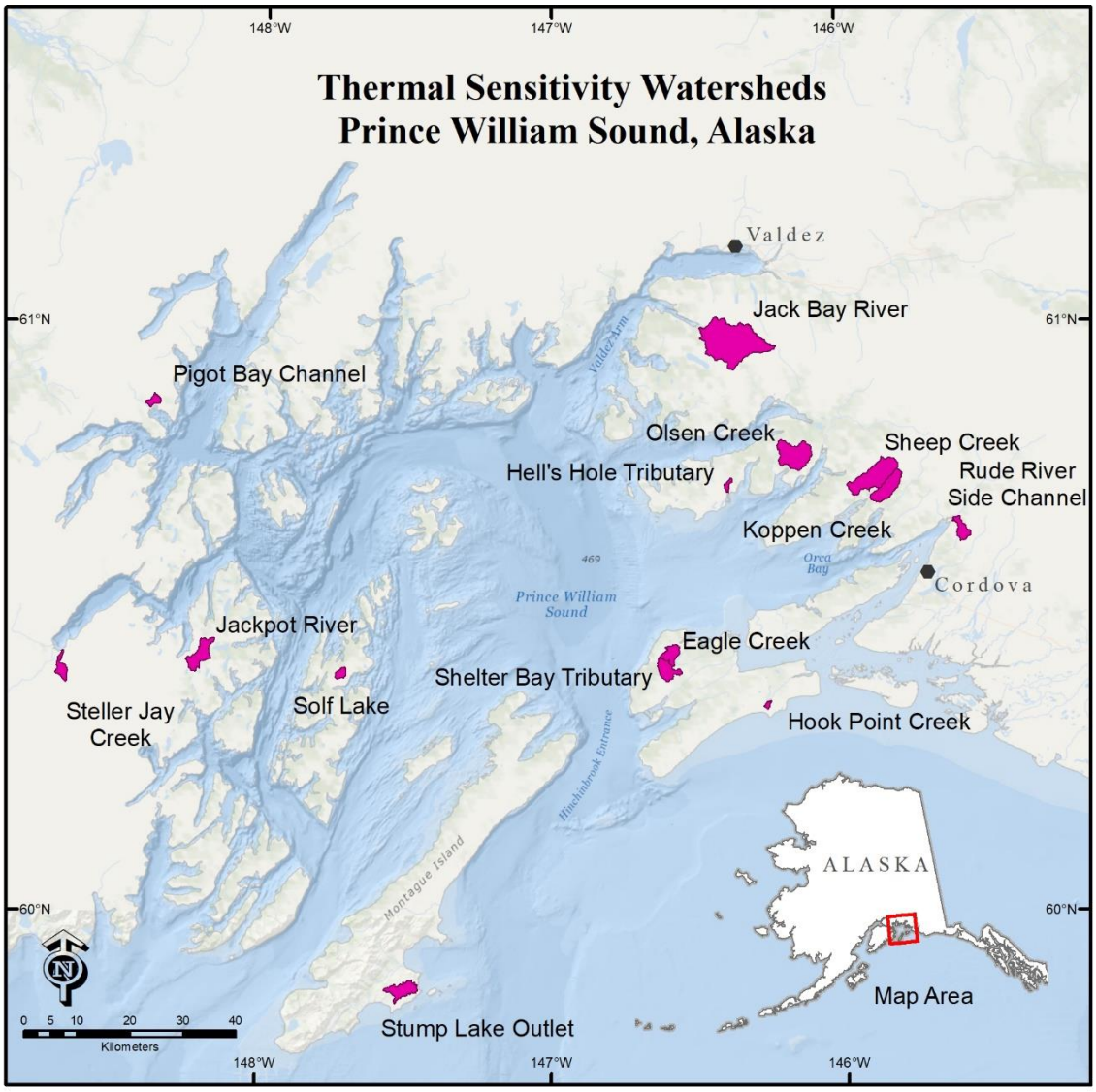


***Figure 1.*** *Watersheds above the 15 monitoring sites in Prince William Sound, Alaska. Note that two sites are located at Solf Lake and cannot be shown at this scale. One site is located at the primary lake inlet; the other is in a bedrock notch at the lake outlet. See Table 1 for descriptive statistics for each watershed.*

## Results

Direct analyses of the air temperature data showed steep gradients during the winter "incubation period" (here defined as 1 October through 30 April) of Pacific salmon found in the study streams (Chum (*O. keta*), Pink (*O. gorbuscha*), and Coho (*O. kisutch*) and much shallower gradients during the summer (May through September) (Figures 2 and 3 of Appendix A). There were also substantial inter-annual variations in incubation period air temperatures among both sites and climate categories, with water years 2014 and 2017 (WY2014, etc.) tending to be 1.5 to 2.5 degrees colder than WY2015 and WY2016.

We developed this relation to develop a predictive model (Figure 22) to project thermal sensitivities for Hydrologic Unit Code 6 (HUC6) watersheds of Prince William Sound based on features of a watershed (Fig. 2). The results suggest that a 14.3% (34 out of a total of 237 watersheds analyzed) of the watersheds to be moderately to highly likely thermally sensitive, meaning that these watershed are likely to experience increases in temperature during the incubation period.

**Potential impacts of climate change on duration of egg incubation:**

To better anticipate potential climate change impacts on the duration of incubation for Coho Salmon eggs, we modeled incubation during the study period and under the two warming scenarios. Scenario 1 assumed that autumn water temperatures would increase but that snow would continue to accumulate and spring temperatures would increase approximately 1$^{o}$C. Scenario 2 assumed a warm autumn and winter so that water temperatures increased that resulted in a 2.6$^{o}$C increase.

The future warming scenarios corresponded with a significant reduction in duration of incubation. The mean duration of incubation was 57 days shorter under Scenario 1, the warming−snow scenario, as compared to the study period. The eggs of early spawning fish were most affected (a 70 day reduction) while eggs of late spawning fish were least affected (a 41 day reduction), indicating that for Scenarios 1 and 2 water temperatures warmed more in late September and early October than March or April.

Springtime warming was greater under Scenario 2, the warming−no snow scenario, when the mean duration of incubation was reduced by 65 days as compared to the study period. Duration of incubation was nearly identical under the 2 scenarios for the eggs of early spawning fish because alevin were projected to emerge from the gravel during the winter, before melting occurred under the Scenario 1. The offspring of mid spawning fish typically emerged earlier under the Scenario 2 as compared to the Scenario 1, but the difference was not statistically significant. For the offspring of late spawning fish, duration of incubation was significantly reduced under Scenario 2 as compared to Scenario 1.

**Figure 2:** Project thermal sensitivities for Hydrologic Unit Code 6 (HUC6) watersheds of Prince William Sound based on observed stream water sensitivities to changes in observed air temperatures between the water years 2016 (warm) and 2017 (cold).

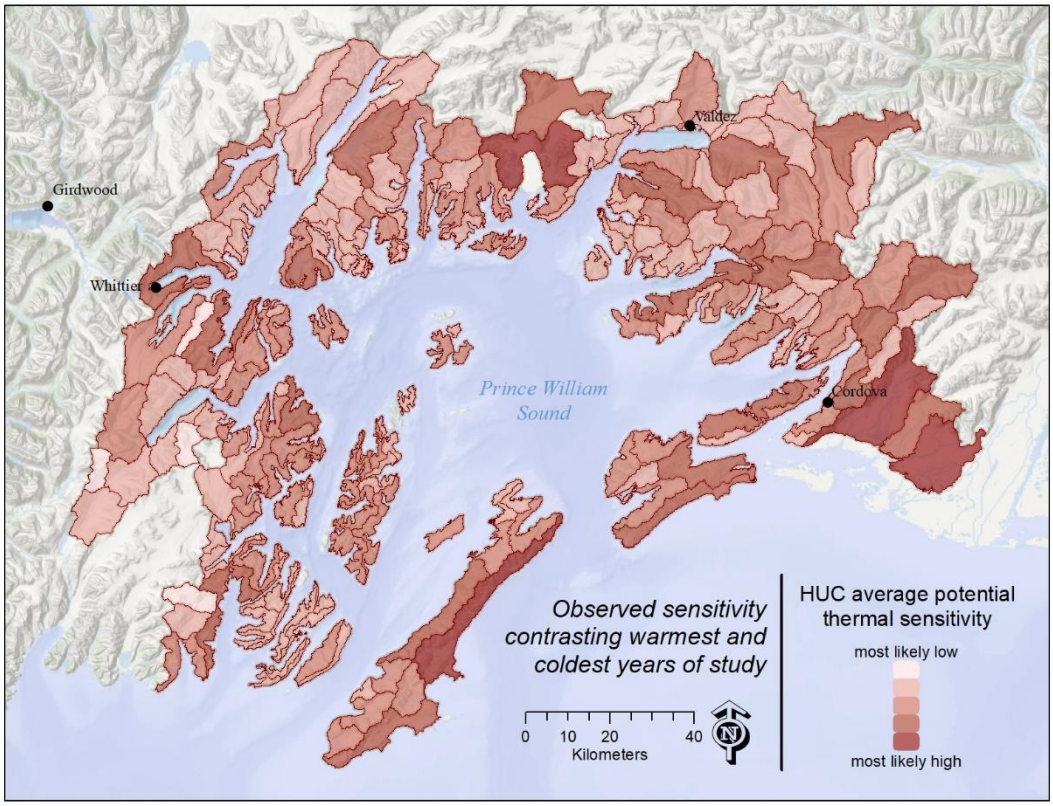


**Implications**

We used the predictive model to project thermal sensitivities for Hydrologic Unit Code 6 (HUC6) watersheds of Prince William Sound. Where HUC boundaries are coincident with the land-ocean interface, the HUC usually includes many smaller, disconnected watersheds, each with its own outlet to the ocean. Thus, the landscape predictor models developed for discrete watersheds give only a general potential thermal sensitivity for all watersheds within each HUC. Individual watersheds might have very different thermal sensitivities.

It is crucial to examine the consequences of changing environmental conditions on a species phenology in order to identify potential mismatches in phenology and better understand effects (Miller-Rushing et al. 2010). Emergence timing is coupled with the availability of the abundance of aquatic invertebrates (Campbell et al. 2019). Changes to thermal and hydrologic regimes that disrupt life-history timing cues can result in mismatches between fish and their environments or food resources, adversely affecting survival (Angilletta et al. 2008, Letcher et al. 2004). Thus, monitoring programs need to be able to detect changes in timing of life-history events to be able to better capture the response to the more nuanced effects of climate change.

If emergence date diverges from optimal conditions, then selection should favor compensatory changes in spawning date or temperature-specific development rate of embryos. Spawning date is likely to evolve, particularly in the short term, owing to its high heritability in salmonids (Quinn et al. 2000; Hard 2004; Hendry and Day 2005; Carlson and Seamons 2008). Changes in egg features and development rate may occur over the longer term because their heritability is lower (Hebert et al. 1998; Kinnison et al. 1998).

There are important ecological implications of climate-related changes in the time and size of fish at emergence. Earlier emergence can result in an extended growing season, a benefit that can lead to increased fitness. Holtby (1988) found that an increase of 1.3 °F (0.7 °C) in winter water

temperatures following timber harvest in Carnation Creek on the west coast of Vancouver Island, British Columbia, resulted in Coho Salmon emerging 6 weeks earlier. Size at age increased because of the extended growing season, resulting in more fish completing their freshwater-rearing life history in one year rather than two. Coho salmon in Carnation Creek also smolted and moved to sea about 2 weeks earlier following timber harvest (which raised stream temperatures); however, marine survival declined, possibly as a result of the decoupling of the timing of smolt migration from marine plankton blooms (Holtby and Scrivener 1989). Similarly, warmer winter temperatures increased the length of the growing season of recently emerged Sockeye Salmon in southwest Alaska. Like Coho Salmon in Carnation Creek, Sockeye Salmon grew faster, and more underwent smolt transformation at age 1+ during warm periods rather than at age 2+ in cooler periods (Schindler et al. 2005). However, age-1+ smolts were smaller than age-2+ smolts and were expected to have decreased marine survival.

Managers and policy makers need to recognize that there are likely to be changes in the time of return of populations, particularly, in the more vulnerable watersheds. This will require potential adjustments in the timing of harvest, monitoring and escapement programs, particularly in the more thermally sensitive watersheds. To ensure that populations have the maximum potential to adapt to changes in their freshwater ecosystems, management should be directed at maintaining and enhancing life-history and genetic diversity not simply focusing on maintaining population numbers.

## Appendix A

## METHODS AND RESULTS:

### Study Area:

The fjords and islands of Prince William Sound (PWS) (Figure 1) form a unique and sheltered inland marine environment entrenched in the exposed northern coastline of the Gulf of Alaska (Mann and Hamilton, 1995). The surrounding terrain is mountainous and high-relief. The highest peak in the area, Mt. Marcus Baker, rises over 4,000 m above sea level in less than 20 km. Tidewater glaciers and large icefields are present on the mainland, particularly along the northern and western coastline where the mountains are highest. Nearly all glaciers in the region have been retreating since the end of the 19$^{th}$ century (Calkin et al. 2001). The islands are de-glaciated, but perennial snowfields persist on north- and west-facing aspects of the highest peaks (600-900 m) on Montague, Hinchinbrook, and Knight Islands.

The surficial geology is most commonly sedimentary or igneous bedrock from the Eocene and Paleocene or unconsolidated glacial deposits from the Holocene and Pleistocene (Wilson et al. 2008). Below 600 m elevation, mature stands of Sitka spruce (*Picea sitchensis*), Mountain hemlock (*Tsuga mertensiana*), and, on the eastern side of PWS, Western hemlock (*T. heterophylla*) are the primary late successional vegetation species (Cooper, 1942). *Sphagnum*- or *Carex*-dominated peatlands, collectively known as "muskegs," are also common and widespread in undisturbed, late successional piedmont areas. Active glacier outwash plains and other disturbed areas are often thickly vegetated with brush, particularly Sitka alder (*Alnus viridis*).

The region's subarctic maritime climate is characterized by cool temperatures, a small annual temperature range, and abundant precipitation (Bieniek et al. 2012). During the 1981-2010 climate period, the mean annual sea level air temperatures were 3 to 5 °C across PWS. Most locations likely received around 200 cm of precipitation at sea level in an average year, with over three times as much precipitation falling at high elevation (Hayward et al. 2017). On a local scale, the influences of mountainous terrain, continental air masses, and glaciers can create steep environmental gradients in temperature and precipitation, particularly in the autumn and winter months (Gay and Vaughan, 2001). For example, Valdez typically receives half as much precipitation as Cordova, located 70 km away (Cooper, 1942). On the regional scale, observed variability in winter temperature and precipitation appears strongly correlated with the strength and position of the Aleutian Low (Bieniek et al. 2012) and sea surface temperature patterns in the North Pacific (Mantua et al., 1997).

The climate is anticipated to warm by 3 °C during the next 50 years (Fresco and Floyd 2017). Importantly, the greatest warming is anticipated in winter, pushing monthly mean air temperatures above freezing year-round near sea level. This warming will increase glacial ablation and reduce low elevation snowpack and seasonal ice cover on lakes and rivers, likely changing freshwater temperature and discharge patterns in PWS.

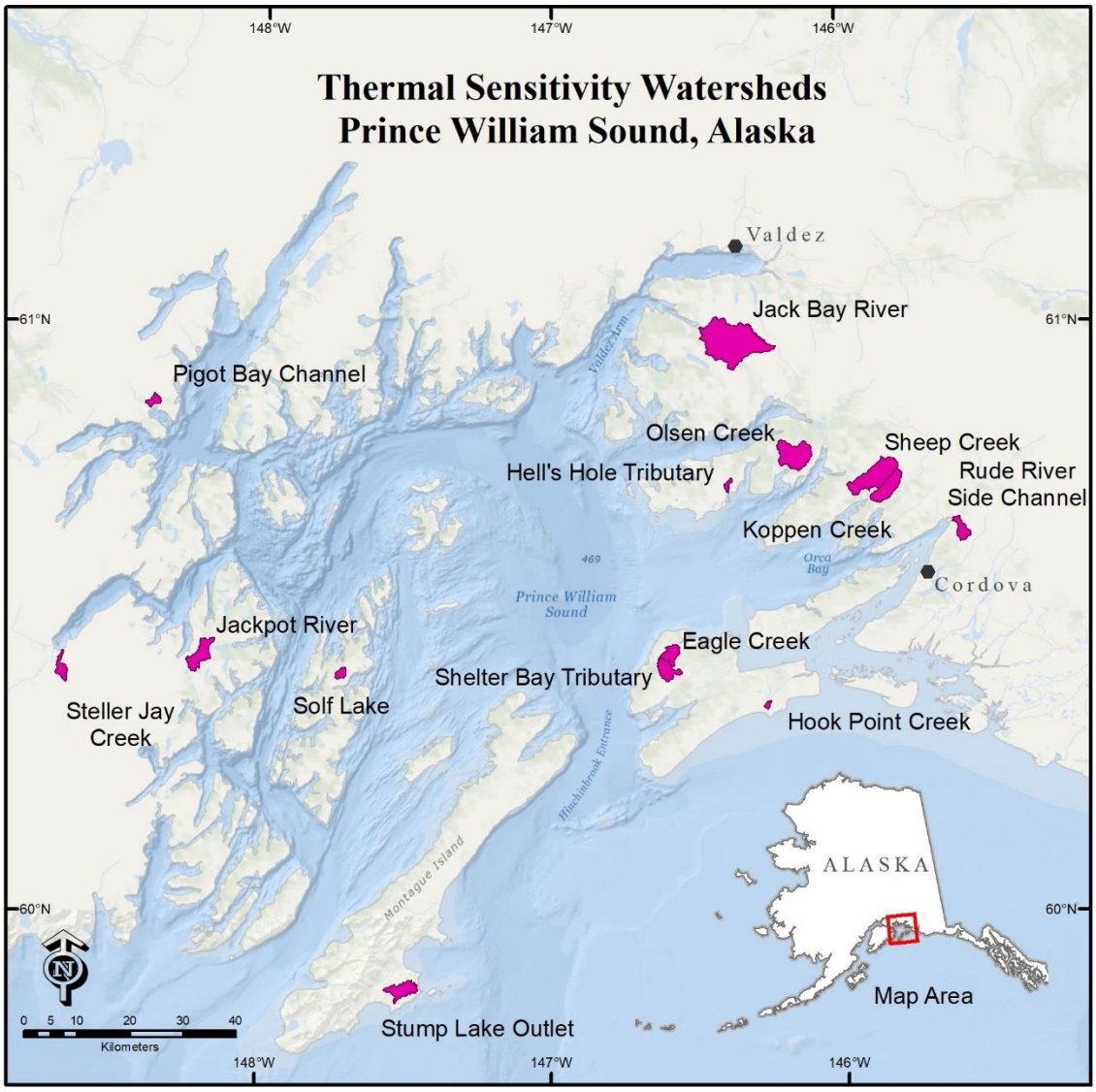


***Figure 1.*** *Watersheds above the 15 monitoring sites in Prince William Sound, Alaska. Note that two sites are located at Solf Lake and cannot be shown at this scale. One site is located at the primary lake inlet; the other is in a bedrock notch at the lake outlet. See Table 1 for descriptive statistics for each watershed.*

**Table 1**: Watershed descriptive metrics for 15 study sites located in Prince William Sound, Alaska.

| Site | Climate Category | Establish Year | Longitude | Lattitude | Area ($km^2$) | Mean Elev (m) | Lakes and Ponds | Perennial Ice and Snow | Woody, Emergent, & Herbaceous Wetlands | Observed Thermal Sensitivity | Best Model Predicted Sensitivity | 7DADA with 4° C warming |
|---|---|---|---|---|---|---|---|---|---|---|---|---|
| | | | | | ($km^2$) | (m) | (%) | (%) | (%) | (°C / °C) | (°C / °C) | (°C) |
| Stump Lake Outlet | Mild | 2013 | 147.45 | 59.87 | 12.26 | 79 | 5 | 0 | 40 | 0.93 | 1.21 | 25.00 |
| Solf Lake Inlet | Cool | 2013 | 147.73 | 60.41 | 3.21 | 310 | 1 | 0 | 0 | 0.13 | 0.40 | 9.26 |
| Solf Lake Outlet | Cool | 2012 | 147.73 | 60.43 | 5.25 | 243 | 12 | 0 | 1 | 0.70 | 0.70 | 18.33 |
| Hook Point Creek | Cool | 2013 | 146.26 | 60.35 | 1.16 | 44 | 0 | 0 | 49 | 1.14 | 0.69 | 12.61 |
| Shelter Bay tributary | Cool | 2012 | 146.64 | 60.43 | 10.65 | 235 | 1 | 0 | 10 | 0.47 | 0.48 | 10.15 |
| Hell's Hole Tributary | Cool | 2013 | 146.39 | 60.72 | 1.79 | 125 | 4 | 0 | 46 | 0.65 | 0.73 | 13.49 |
| Sheep River | Cold | 2013 | 145.90 | 60.72 | 30.88 | 638 | 1 | 15 | 0 | 0.22 | 0.35 | 11.85 |
| Eagle Creek | Cold | 2013 | 146.57 | 60.46 | 8.33 | 79 | 1 | 0 | 41 | 0.56 | 0.72 | 14.47 |
| Koppen Creek | Cold | 2013 | 145.90 | 60.71 | 16.44 | 413 | 0 | 0 | 0 | 0.43 | 0.34 | 8.25 |
| Rude River Side Channel | Cold | 2013 | 145.61 | 60.66 | 7.31 | 597 | 2 | 21 | 6 | 0.22 | 0.24 | 9.57 |
| Olsen Creek | Cold | 2013 | 146.18 | 60.76 | 25.68 | 417 | 0 | 1 | 1 | 0.49 | 0.48 | 9.84 |
| Jack Bay River | VCold | 2013 | 146.47 | 61.00 | 73.00 | 632 | 0 | 12 | 0 | 0.50 | 0.52 | 10.19 |
| Pigot Bay Channel | VCold | 2013 | 148.40 | 60.86 | 3.75 | 254 | 0 | 1 | 2 | 0.23 | 0.07 | 5.36 |
| Steller Jay Creek | VCold | 2016 | 148.68 | 60.44 | 6.29 | 629 | 0 | 20 | 0 | | 0.29 | |
| Jackpot River | VCold | 2013 | 148.25 | 60.42 | 14.70 | 260 | 6 | 0 | 3 | 0.25 | 0.53 | 17.59 |
| AVERAGE = | | | | | 14.71 | 330 | 2 | 5 | 13 | 0.49 | 0.52 | 12.57 |

**Study Catchment Characteristics:**

We established 15 monitoring locations at known salmon spawning sites in PWS during the summer of 2013 (Figure 1). The study watersheds range from the Gulf of Alaska coast on Montague and Hinchinbrook Islands, to large glaciated mainland watersheds draining into northern PWS. The watersheds were distributed from east-to-west, across the PWS climate gradient.

The watershed selection was not made randomly. Rather, we knew that we only had sufficient resources to sample a relatively small number of watersheds, and we wanted to make sure that our sample included much of the range of watersheds present in PWS, by size, elevation, locations, and land cover. We attempted to pick smaller groups of watersheds that would allow for comparisons within the group that might be related to their potential sensitivity to climate change. A critical factor was the winter mean temperature and the likely shift from snow dominated, to rain-on-snow dominated, to rain dominated under a future warmer climate (Figure 2). We explicitly built these factors into our site selection.

We first examined distributed temperature data in order to estimate the likely elevational boundaries of the rain-on-snow zone and divided PWS into three zones: 1) the outer-coastal zone consisting of the large, outer islands of Montague and Hinchinbrook; 2) a central sound zone, north to south, including both islands and deep mainland bays, but excluding large glaciated mainland systems and the outer-coastal islands; and 3) a mainland zone consisting primarily of large, glacially dominated watersheds. We then analyzed the distribution of watershed area within each watershed, divided into 50-m elevation bands in order to classify the climate regime for each group of watersheds.

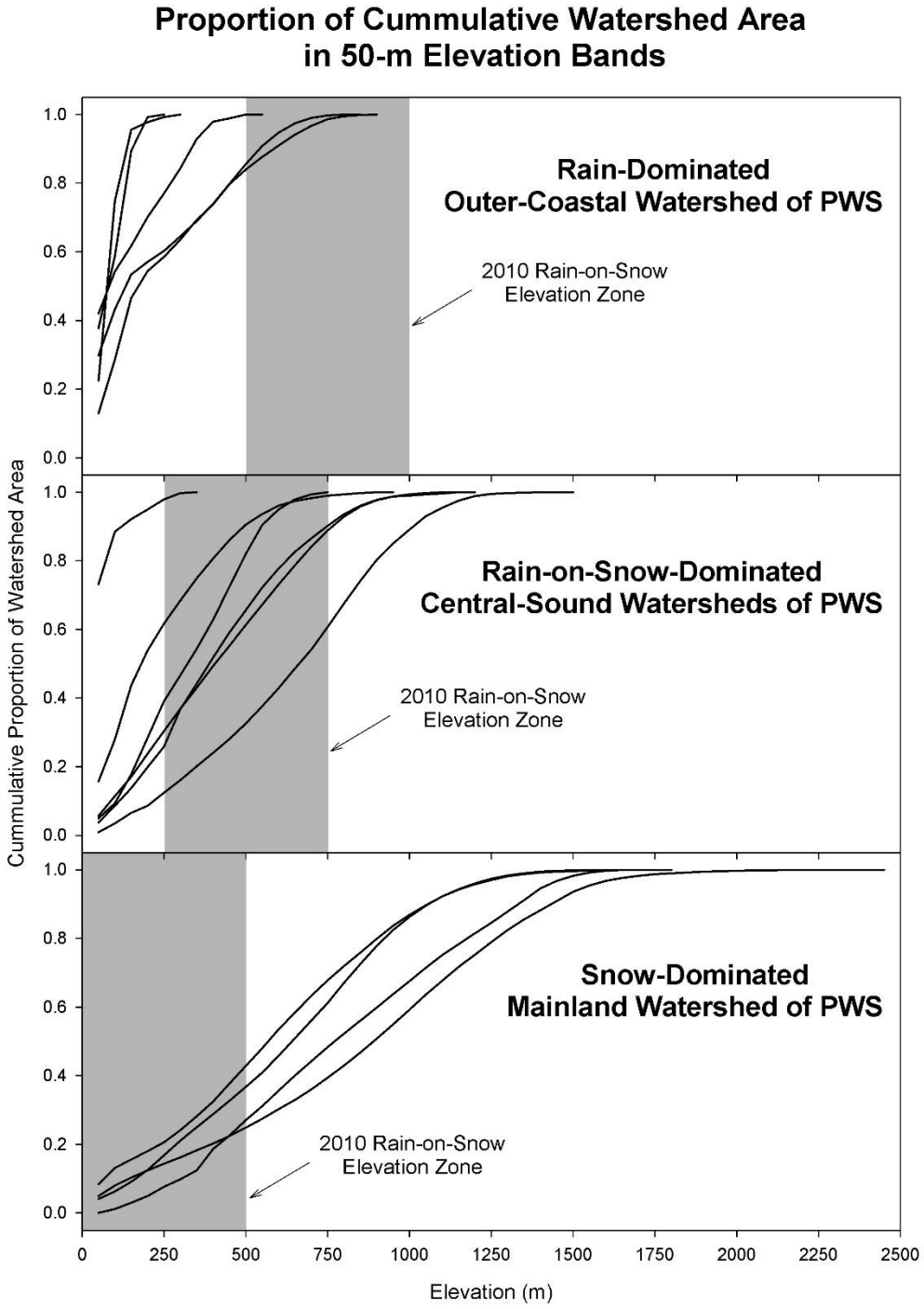


*Figure 2. Hypsometric curves showing the cumulative distribution of watershed area falling across 50-m elevation zones. The present-day rain-on-snow zone is indicated with gray shading. Watersheds within each geographic zone have similar winter climate, except for Hell's Hole, a small, lowland-dominated watershed in the central sound that was rain dominated.*

**Temperature Data Collection:**

We collected hourly air temperature and surface (stream) and shallow streambed water temperature data from 1 October, 2013 until 1 October, 2017. We recorded air temperature with a HOBO Pendant data logger housed in a gill radiation shield produced by the Onset Computer Corporation. We recorded surface water temperature at the bottom of the water column with 1 HOBO Pro v2 data logger housed in a 15-cm-long section of 4.1-cm internal diameter galvanized steel pipe to shade the sensor and protect it from physical damage. Deployment depths were at least 20 cm, typically 50 to 60 cm, at average summer water flows and the surface water at each study site was assumed to be well mixed by turbulent flow.

We measured streambed water temperature 35 to 50 cm into the streambed using a TidbiT v2 data logger installed directly into the substrate after boring a hole with a custom-made driver (Zimmerman and Finn 2012). We deployed two streambed loggers at each site. Burial depth for Coho Salmon eggs ranges between 8 and 55 cm and is correlated with size of the maternal female (van den Berghe and Gross 1984; DeVries 1997). By measuring water temperature at the stream bottom and up to 50 cm into the streambed, we bracketed the potential range of incubation temperature experienced by eggs at each location.

We downloaded data loggers every 6 to 12 months throughout the study period. We removed erroneous values, including unreasonable outliers (which suggest sensor error) and abnormally high hourly variance (>3°C), suggesting the sensor was exposed to air. Occasional data gaps occurred when streambed data loggers were exposed to surface water, surface water loggers were exposed to air, and when data loggers were lost, malfunctioned, or were not downloaded in 2018. The most prolific data gaps were for air temperature. Cold winter air temperatures reduced battery longevity, resulting in data logger failure in many cases.

Using hourly temperature data, excluding days with fewer than 24 measurements, we calculated daily mean temperature for each data-logger location at each site. We calculated weekly (7-day, “non-rolling”) and monthly mean temperatures for surface-water temperatures at each site from the daily mean temperature, excluding weeks with fewer than seven days of data and months with fewer than 28 days of data.

**Analysis of Air Temperature Gradients:**

The first step in our analysis of streams' thermal sensitivity to changing air temperatures was to compile a time series of air temperatures that we could relate to each site where we measured water temperature. While we did install air temperature loggers at each site, missing data would have prevented a complete analysis of our stream temperature data if we restricted that analysis to only air temperatures co-recorded at each site. Therefore, we needed to identify sites with similar air temperature regimes that could be averaged together to provide a master record of air temperatures. Further, because winter air temperatures exhibit steep environmental gradients within Prince William Sound, we did not want to use a single station with a long and complete record (e.g., NOAA's Cordova Station) to analyze water temperatures across all sites.

We analyzed mean weekly air temperatures over the winter of 2016-17 because this was the winter for which we had the fewest sites with missing air temperature data. We also included data from 3 NOAA weather stations in this analysis, and the data from the Cordova and Valdez stations were later used to augment our site data. Solf Lake data were missing so we repeated the PCA analyses using the winter weekly air temperatures from 2013-14, and then conducted a simple linear regression to relate the mean PCA scores from Solf Lake with the other sites. This regression was then used to back-fill the Solf Lake's PCA loadings on the first and second eigenvectors (Figure 1). Following these analyses, we subdivided our sites into 4 climate categories based on uniformly spaced intervals along the PC1 axis (mild, cool, cold, and very cold) and generated mean weekly air temperatures for each climate category (Figure 1).

Direct analyses of the air temperature data showed steep gradients during the winter "incubation period" (here defined as 1 October through 30 April) and much shallower gradients during the summer (May through September) (Figures 2 and 3). There were also substantial inter-annual variations in incubation period air temperatures among both sites and climate categories, with water years 2014 and 2017 (WY2014, etc.) tending to be 1.5 to 2.5 degrees colder than WY2015 and WY2016 (Tables 1 and 2). The incubation period was also characterized by large week-to-week variation in air temperature, in all years, with alternating freeze and thaw events, even in the middle of winter (Figure 3).

**Figure 3:** Principle component analysis of air temperature gradients across Prince William Sound with the range of sites on PC1 divided into 4 equal length categories (boundaries noted by vertical dashed lines); gray shaded regions were not included when determining the category boundaries. Data from NOAA's Cordova (Co-op ID: 998425) and Valdez (Co-op ID: 702756) weather stations were included with the field sites because the Stump Lake site and all the very cold sites had frequent missing data. NOAA's Bligh Reef site (Co-op ID: 994680) was included in the PCA, but not used in subsequent analyses.

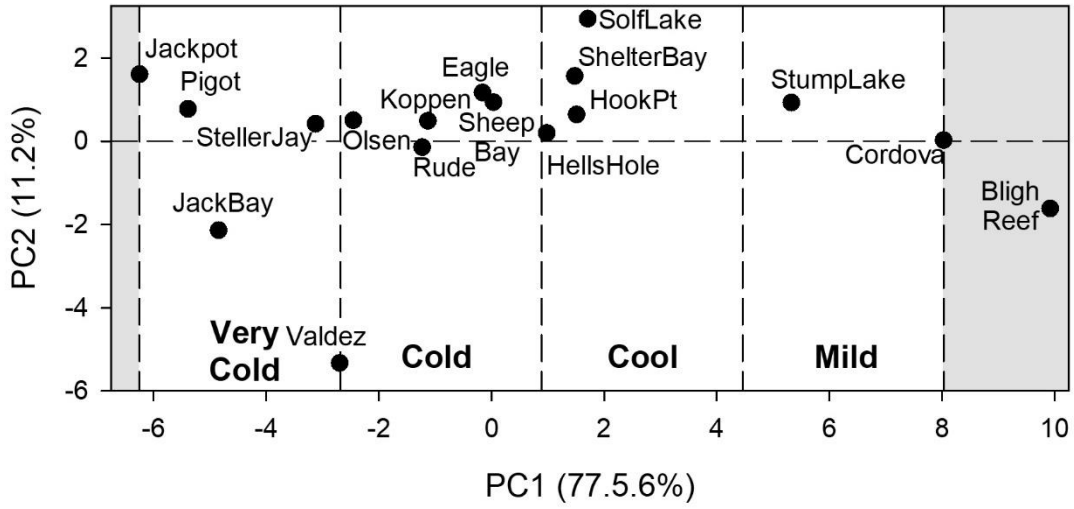

**Figure 4:** Relationship between the first principle component and air temperature averaged for each site over the summer (May through September) and the incubation period (October through April) Points and x-axis are as in Figure 1 and also include both NOAA's Bligh Reef station (Co-op ID: 994680).

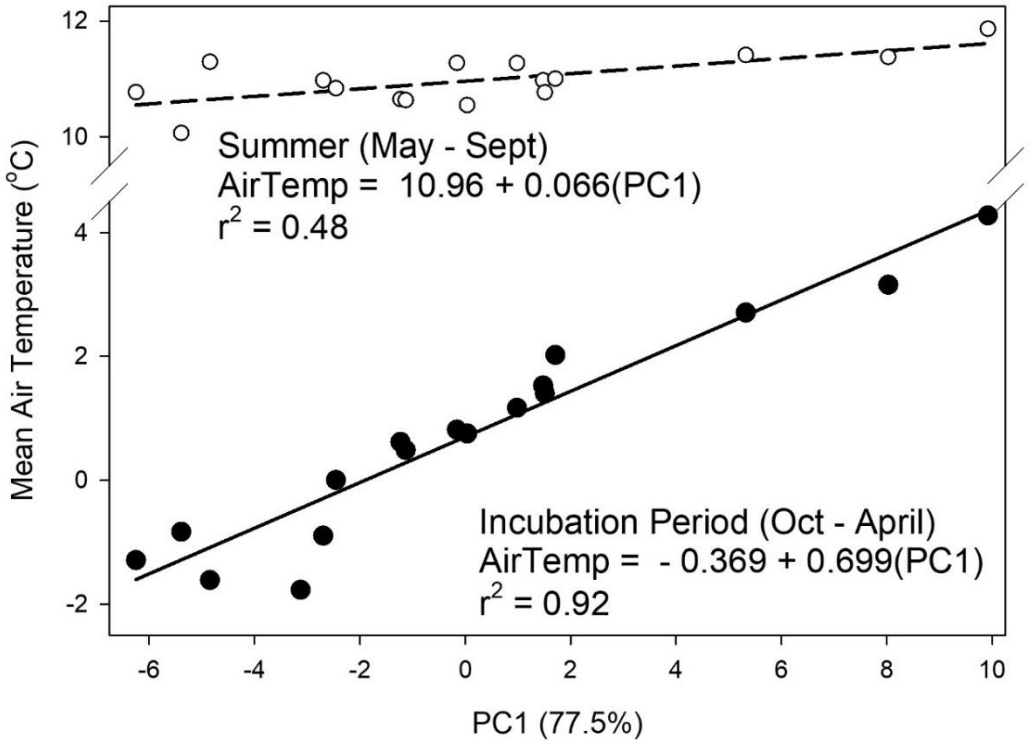

**Figure 5:** Time series of weekly air temperatures averaged for the sites falling in each climate category shown in Figure 1. See also Table 2.

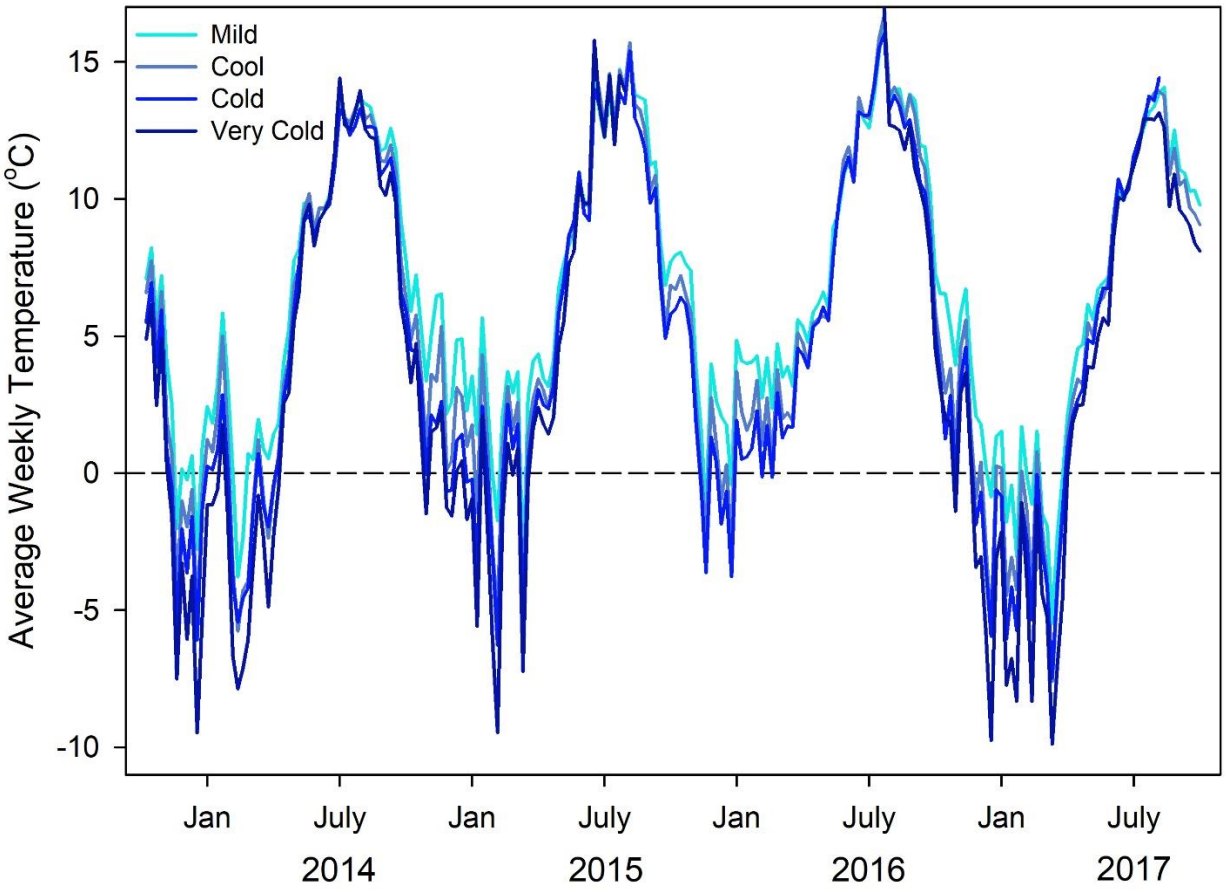

**Table 2**: Mean incubation period air temperatures from 3 NOAA weather stations and 14 study sites located throughout Prince William Sound. Although averages are given for each year with incubation period data, some years will include missing data which may somewhat distort the reported average. Some sites had no data within the incubation period of a given year so no value is reported (-). Sites are categorized based on a PCA analysis and ranked from warmest (Stump Lake) to coldest (Jackpot Lakes) (Figure 1).

| Site | Coop-ID Category | 2014 | 2015 | 2016 | 2017 | All-Year Mean |
|---|---|---|---|---|---|---|
| Bligh Reef | 994680 | 2.60 | 6.23 | 5.42 | 2.85 | **4.27** |
| Cordova | 998425 | 2.39 | 3.69 | 4.34 | 2.21 | **3.16** |
| Valdez | 702756 | -1.77 | -0.44 | 0.31 | -1.69 | **-0.90** |
| Stump Lake | Mild | 1.85 | 3.35 | 4.12 | 1.51 | **2.71** |
| Solf Lake | Cool | 0.49 | 1.60 | 2.67 | 3.33 | **2.02** |
| Hook Point | Cool | 0.59 | 2.27 | 2.73 | -0.01 | **1.40** |
| Shelter Bay | Cool | 0.53 | 2.29 | 3.20 | 0.10 | **1.53** |
| Hells Hole | Cool | 0.41 | 1.67 | 2.74 | -0.14 | **1.17** |
| Sheep Bay | Cold | -0.06 | 1.33 | 2.20 | -0.45 | **0.75** |
| Eagle Creek | Cold | 0.04 | 1.02 | 2.66 | -0.46 | **0.82** |
| Koppen Bay | Cold | -0.13 | 1.12 | 1.84 | -0.88 | **0.49** |
| Rude River | Cold | - | 0.94 | 1.96 | -1.06 | **0.62** |
| Olsen Bay | Cold | -0.72 | 0.45 | 1.62 | -1.35 | **0.00** |
| Steller Jay Ck | V. Cold | - | - | - | -1.77 | **-1.77** |
| Jack Bay | V. Cold | -1.72 | -0.56 | -1.76 | -2.42 | **-1.62** |
| Pigot Bay | V. Cold | -1.32 | -0.36 | 0.82 | -2.48 | **-0.83** |
| Jackpot Lakes | V. Cold | -2.01 | -0.06 | -0.33 | -2.76 | **-1.29** |
| **All-Site Mean** | | **-0.17** | **1.16** | **1.88** | **-0.63** | **0.43** |

**Table 3**: Mean incubation period air temperatures by temperature category (Figure 1) based on the 14 study sites located throughout Prince William Sound and data from the Cordova and Valdez weather stations. Although averages are given for each year, some years will include missing data which may somewhat distort the reported average.

| Category | 2014 | 2015 | 2016 | 2017 | All-Year Mean |
|---|---|---|---|---|---|
| **Mild** | 2.28 | 4.01 | 4.63 | 2.19 | **3.28** |
| **Cool** | 0.50 | 1.96 | 2.83 | 0.01 | **1.33** |
| **Cold** | -0.22 | 0.96 | 2.05 | -0.84 | **0.49** |
| **V. Cold** | -1.75 | -0.35 | 0.27 | -2.22 | **-1.01** |

**Thermal Sensitivity Analyses:**

The sensitivity of stream temperatures during the incubation period to changes in air temperature was evaluated in several ways. First, we compared the observed differences in weekly means of the climate category mean air temperature with the stream temperature observed at each site. We focused our comparison between the coldest (WY2017) and warmest (WY2016) years that occurred during our study.

The relationship between mean weekly air temperature and mean weekly surface (or stream) water temperature was also analyzed with a variety of regression models. We started with a 4-parameter logistic regression (Mohseni et al., 1998) and tested the model's ability to predict average daily water temperature during the incubation period. At a few sites, the logistic equation failed to converge to a solution – where stream temperatures appeared to be strongly controlled by groundwater and the "S-shaped" logistic curve could not be reasonably fit to the data. Also, analysis of residuals suggested temperature at many sites displayed hysteresis, such that spring-time water temperatures were colder than autumn water temperatures at any given air temperature. Consequently, all sites were modeled in 4 ways: 1) non-hysteretic logistic equation; 2) hysteretic logistic equation; 3) non-hysteretic linear regression; and 4) hysteretic linear regression. Our study focused on the winter, or incubation period, thus, for each site, we tested the models' ability to accurately predict observed water temperatures from the observed air temperatures over the incubation period.

We used the Nash-Sutcliffe model efficiency coefficient (NSC; Mantua et al., 2010) to test the model fit by comparing observed versus predicted daily mean surface water temperature over the duration of the incubation period. Note first that this is a rigorous test, focusing on daily mean temperatures over the winter when streams were often frozen. Also note that models fit to full-year water temperatures, that is, including the summer, usually had much higher NSC (results not shown). Finally, we also analyzed the thermal sensitivity for periods when weekly mean air temperatures were above zero (Kelleher et al. 2012).

For each site, we then selected the best model (Figures 6 & 7), based on the NSC objective function (Table 4), and using that model, we predicted daily average water temperatures under a warmer air regime by adding 4 °C to the daily average air temperature for each day of the record in each of the 4 years of the study. We then divided the change in predicted water temperature (predicted from observed air temperature versus predicted from 4 °C warmer air temperature) by 4 to express the thermal sensitivity as the change in water temperature for each degree C change in air temperature (°C/°C; Table 5). The observed thermal sensitivity between WY2016 and WY2017 was treated similarly, however the change in the air temperature between years was calculated from the average climate category air temperature. The slope of the linear regressions did not need to be normalized as it was already in the desired units (°C/°C).

**Table 4:** Model fit statistics comparing observed versus predicted daily mean water temperature over the duration of the incubation period based on the Nash-Sutcliffe model efficiency coefficient (NSC). The best model fits will have NSC=1. Bold text indicates the best model at each site. The 4-parameter logistic (logistic) model did not converge (DNC) to a solution at three sites.

| | Logistic non-hysteretic | Logistic HYSTERETIC | Linear non-hysteretic | Linear HYSTERETIC |
|---|---|---|---|---|
| Site | NSC | NSC | NSC | NSC |
| Eagle | 0.67 | **0.72** | 0.52 | 0.55 |
| HellsHole | **0.71** | **0.71** | 0.59 | 0.59 |
| HookPt | 0.50 | **0.57** | 0.42 | 0.48 |
| JackBay | 0.67 | **0.69** | 0.55 | 0.55 |
| Jackpot | 0.49 | **0.77** | 0.38 | 0.55 |
| Koppen | 0.71 | **0.75** | 0.67 | 0.71 |
| Olsen | 0.64 | **0.77** | 0.58 | 0.69 |
| Pigot | 0.26 | DNC | 0.25 | **0.69** |
| Rude | DNC | DNC | 0.26 | **0.66** |
| Sheep | DNC | DNC | 0.56 | **0.76** |
| ShelterBay | 0.59 | **0.69** | 0.53 | 0.63 |
| Solf | 0.25 | **0.56** | 0.17 | 0.45 |
| SolfOutlet | 0.34 | **0.53** | 0.26 | 0.38 |
| StumpLake | 0.65 | **0.66** | 0.60 | 0.60 |
| AVERAGE | 0.54 | 0.68 | 0.45 | 0.59 |

**Figure 6:** Example of the 4-parameter logistic equation using weekly average air temperature to predict the weekly average surface, or stream, temperature for Olsen Bay Creek. Yellow symbols denote the period of spring-time warming, from beginning of February through the end of June; blue symbols denote the period of autumn cooling, from the beginning of July through the end of the following January.

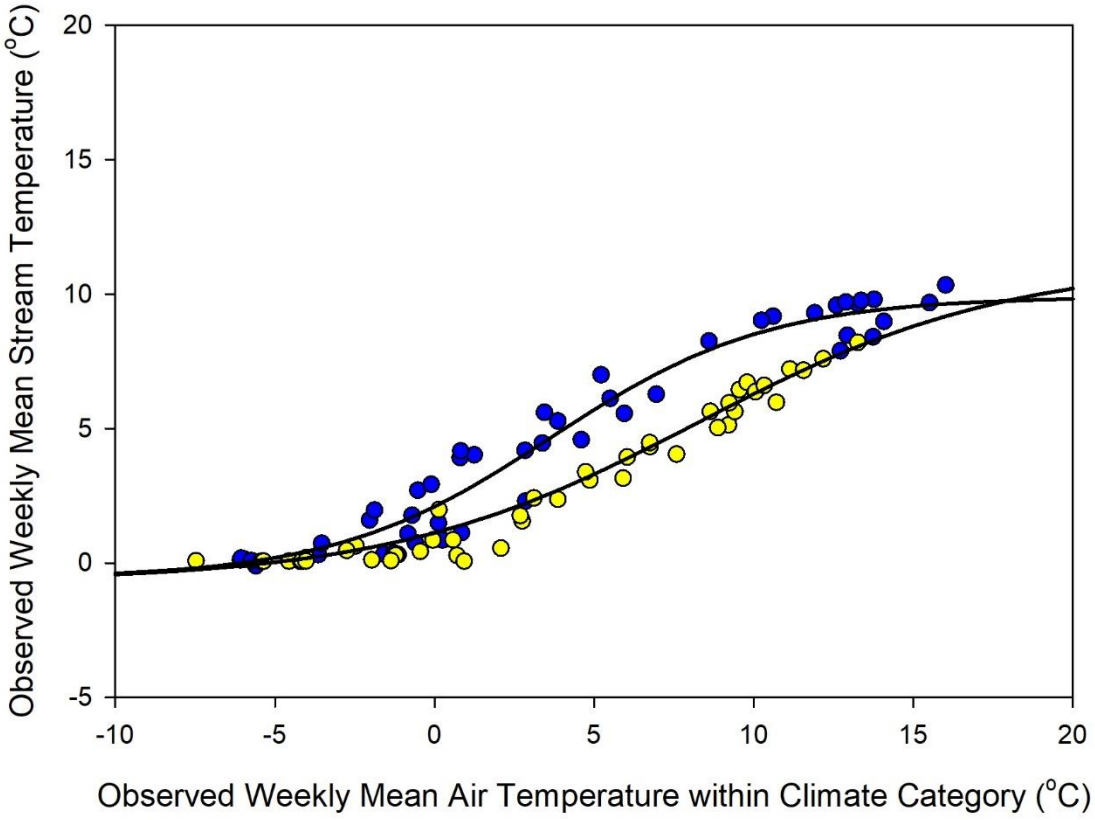

**Figure 7:** Example of the linear regression equation using weekly average air temperature to predict the weekly average surface, or stream, temperature for Pigot Bay Creek. Note that the logistic equation would not converge to a solution for this site and two other sites (Rude River and Sheep Creek). Consequently, the linear regression was used. Symbol colors as in Figure 6.

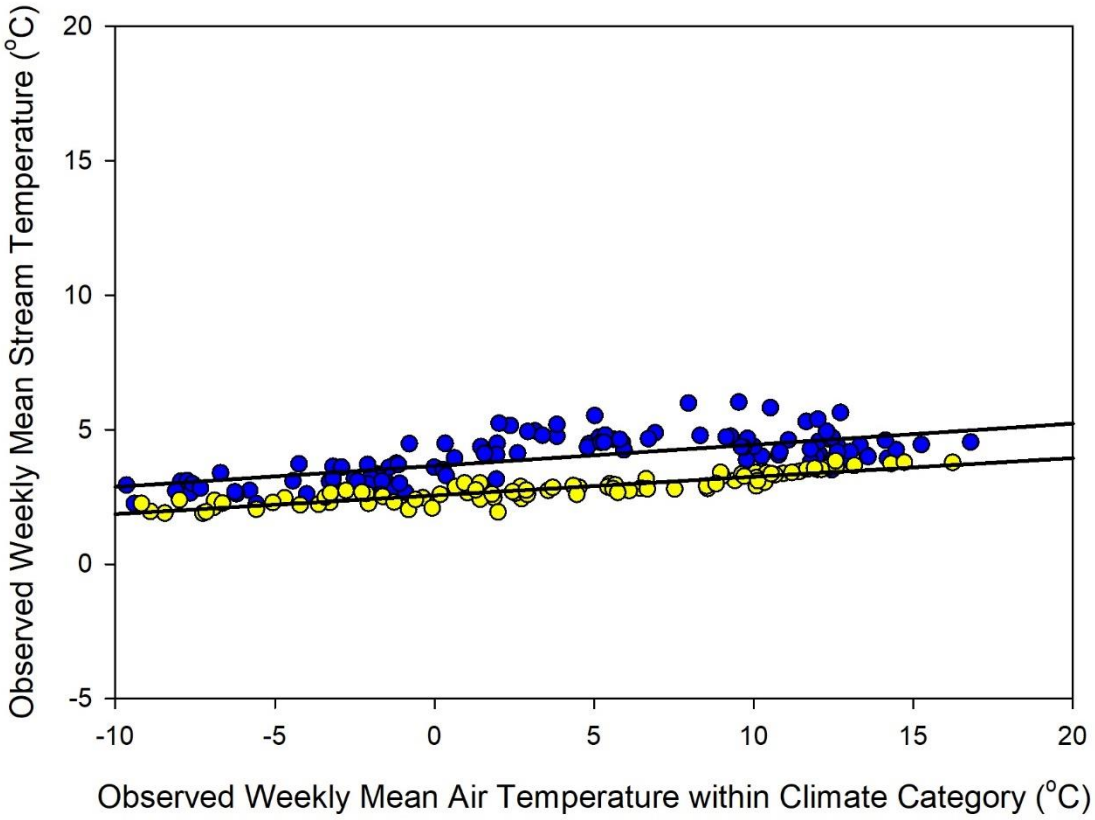

**Table 5:** Summary of stream water thermal sensitivity to changes in air temperature. To simplify comparison among sites and metrics, the thermal sensitivity was normalized by the change in air temperature and expressed as the change of water temperature, in degrees C for a 1-degree C change in air temperature (°C/°C). Thermal sensitivities were analyzed separately for the entire incubation period versus the mid-winter period.

| | | Incubation Period (October - April) | | |
|---|---|---|---|---|
| | | Observed | NSC on mean daily temp | Linear non-freezing |
| Site | Climate Category | (°C / °C) | (°C / °C) | (°C / °C) |
| StumpLake | Mild | 0.93 | 1.21 | 1.34 |
| Solf | Cool | 0.13 | 0.40 | 0.50 |
| SolfOutlet | Cool | 0.70 | 0.70 | 1.00 |
| HookPt | Cool | 1.14 | 0.69 | 0.77 |
| ShelterBay | Cool | 0.47 | 0.48 | 0.55 |
| HellsHole | Cool | 0.65 | 0.73 | 0.86 |
| Sheep | Cold | 0.22 | 0.35 | 0.38 |
| Eagle | Cold | 0.56 | 0.72 | 0.93 |
| Koppen | Cold | 0.43 | 0.34 | 0.36 |
| Rude | Cold | 0.22 | 0.24 | 0.25 |
| Olsen | Cold | 0.49 | 0.48 | 0.55 |
| JackBay | VCold | 0.50 | 0.52 | 0.47 |
| Pigot | VCold | 0.23 | 0.07 | 0.07 |
| Jackpot | VCold | 0.25 | 0.53 | 1.01 |
| | AVERAGE = | 0.49 | 0.53 | 0.65 |

**Exploring Landscape Predictors of Thermal Regimes and Thermal Sensitivity:**

The analyses described above generated a large list of potential temperature metrics that could be used to described both the current thermal regime (including the mean and variance for both the full incubation period and the three mid-winter months (December-February) for the minimum, mean, and maximum daily air temperatures; counts of days during the incubation period when water temperatures exceeded 2 °C (warm days) or were below 0.5 °C (cold days)) and each watershed's thermal sensitivity (described above) which was calculated for both the full incubation period and the 3 mid-winter months. Many of these metrics were highly correlated, suggesting that time-consuming analysis of each metric would be redundant. To narrow the list of metrics, we conducted a Principle Component Analysis (PCA) from which we selected a number of thermal metrics for further analysis. Our first PCA showed that metrics based on the minimum, mean, and maximum daily air temperatures were always highly correlated so the minimum and maximum metrics were dropped from the analysis and the PCA was repeated (Figure 8).

We also derived a large number of potential predictor variables from available GIS coverages of the Prince William Sound area. The outline of each watershed above our study sites was delineated from the U.S. Geological Survey (USGS) 5-m interferometric synthetic aperture radar (IFSAR) 5m digital elevation model (DEM) using spatial analyst tools in ArcGIS 10.5 (Environmental Systems Research Institute, Redlands, CA, USA). Catchment lake and stream coverage was calculated with data from the USGS National Hydrography Dataset (U.S. Geological Survey, 2013). Land cover (vegetation) statistics were calculated using the USGS National Land Cover Database (NLCD) (Homer et al. 2015). Surficial geology statistics were calculated using geologic mapping data from USGS [*Wilson et al.*, 2008]. The geologic layers needed to be simplified and combined because, often, just one or two watersheds would include some area of a given geologic mapping unit. Further details are given in Table A1, in the appendix. Some of the NLCD metrics were also combined, as follows: both woody-wetlands and emergent (herbaceous) wetlands as "wetlands"; grass and sedge dominated areas as "grassy".

Many of the landscape predictor metrics were highly correlated, and would thus violate assumptions of independence in subsequent parametric multiple linear regressions. To narrow the list of potential variables, we conducted a PCA and selected a subset of variables to be used in subsequent analyses. We conducted a first PCA and used those results to eliminate a large number of potential variables and then used the remaining variables in a final PCA (Figure 9).

In general, the PCA analysis of the watershed predictor variables showed relatively weak explanatory power, with the first two eigenvectors explaining only 49.2% of the total variation in the dataset (Figure 8). Large watersheds that included high elevation areas with relatively high proportion of the watershed area in glaciers or perennial snow tended to fall toward the right side of the first axis (PC1). Those watersheds also had large proportion of their areas dominated by barren (unvegetated) or grassy vegetation and had relatively high annual precipitation. Small watersheds with lower elevation and higher annual mean temperatures tended to fall toward the left on PC1. Those watersheds also had an abundance of lakes, wetlands, and coniferous forest (Figure 9)

**Figure 8:** Final PCA on reduced list of potential temperature metrics. Abbreviations are as follows: INC=incubation period; DJF=December, January, and February; ObsSens=observed thermal sensitivity; NSCSens=best model using the Nash-Sutcliffe Coefficient objective function; ATUSens=best model using the ATU objective function; SUMSens=summer (non-freezing air temperature) linear sensitivity.

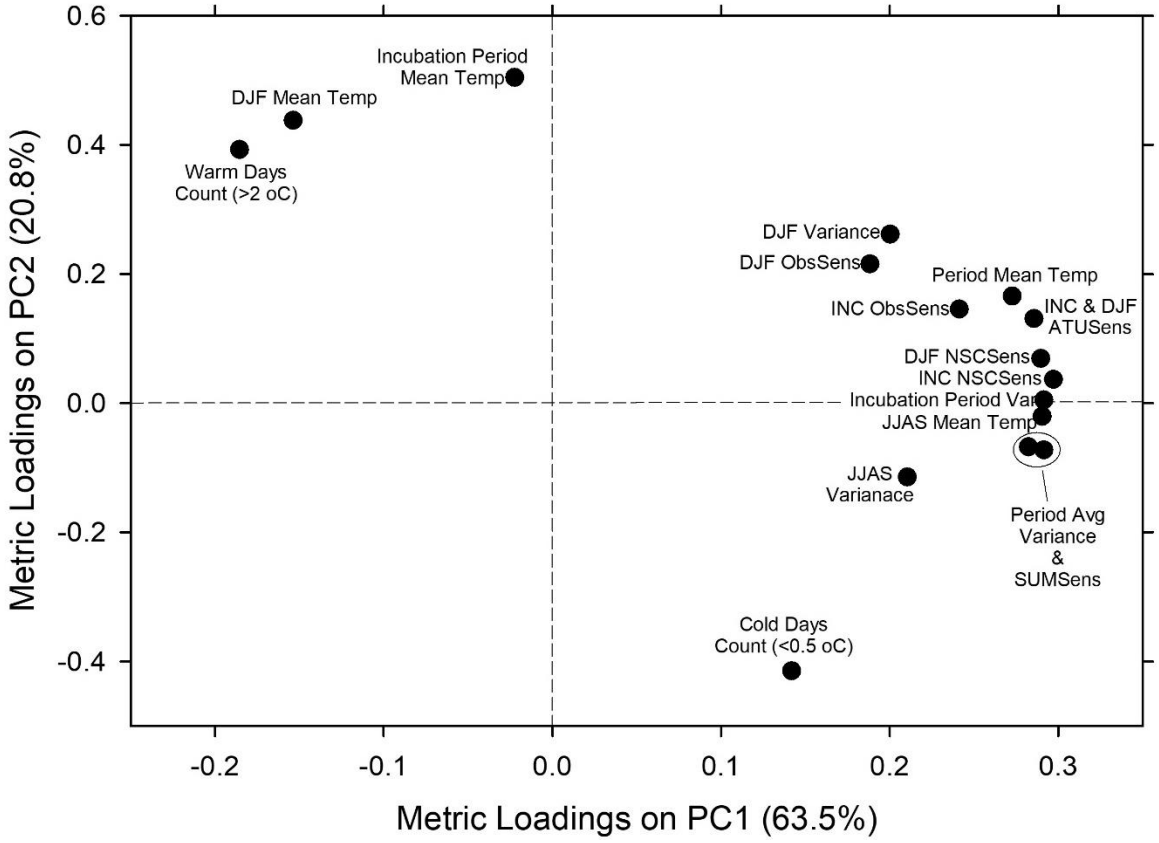

**Figure 9:** Final PCA on reduced list of potential predictor variables derived from various GIS layers available for the study site. Abbreviations are as follows: PPT=PRISM derived precipitation; Temp=PRISM derived temperature; Till=glacial drift and deposits; Glacial=perennial ice and snow cover; Lakes=Lakes, ponds, and streams.

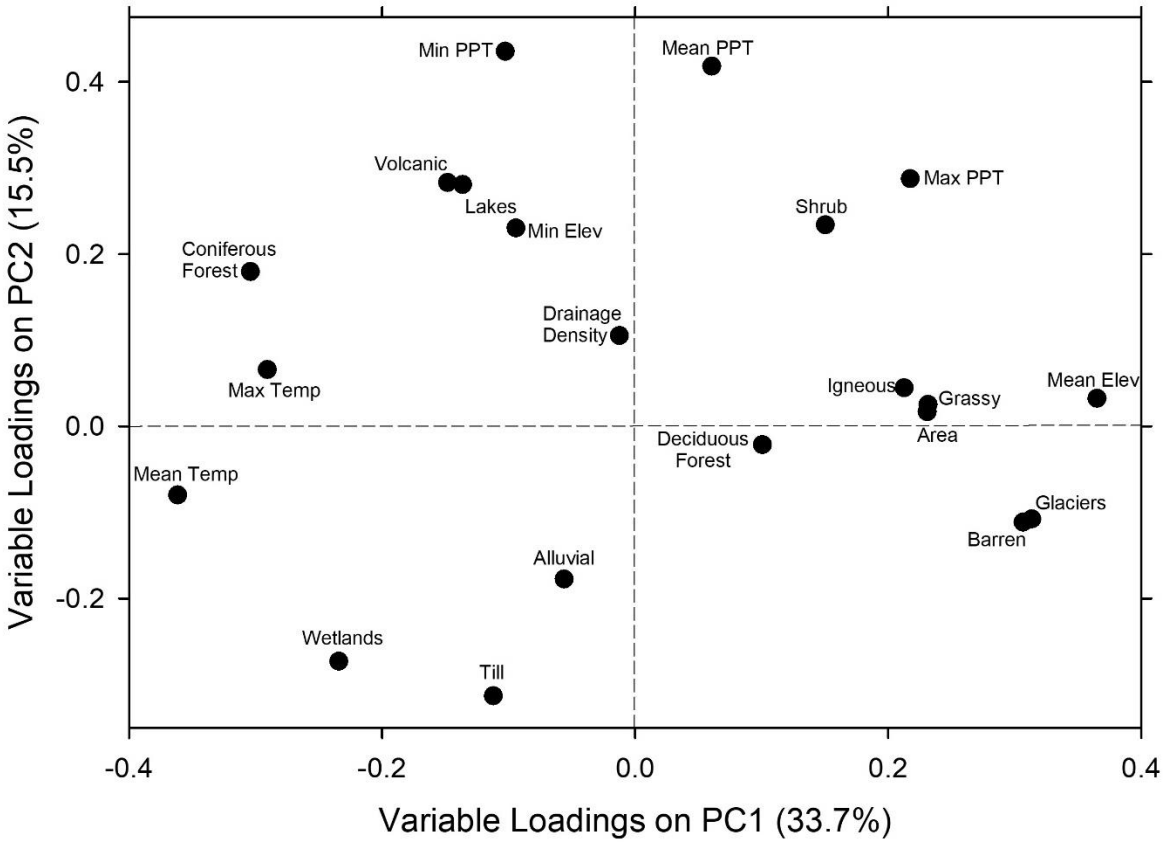


We used linear regression to relate thermal metrics to landscape variables. We first compared each watersheds score on PC1 with the thermal sensitivity observed between the warmest (WY2016) and coldest (WY2017) years. PC1 was a poor predictor of the watersheds' thermal sensitivity (Figure 10A). Overall, the regression model using PC1 to predict thermal sensitivity over predicted the sensitivity of groundwater dominated streams that were relatively insensitive to changes in air temperature and under predicted the sensitivity of streams with large shallow lakes in their watersheds and where observed thermal sensitivity was high (Figure 10B).

**Figure 10: A)** Regression fit between final PCA scores for each site and that site's observed thermal sensitivity, and **B)** fit between observed thermal sensitivity and the sensitivity predicted from a simple linear regression model using PC1 as the predictor variable.

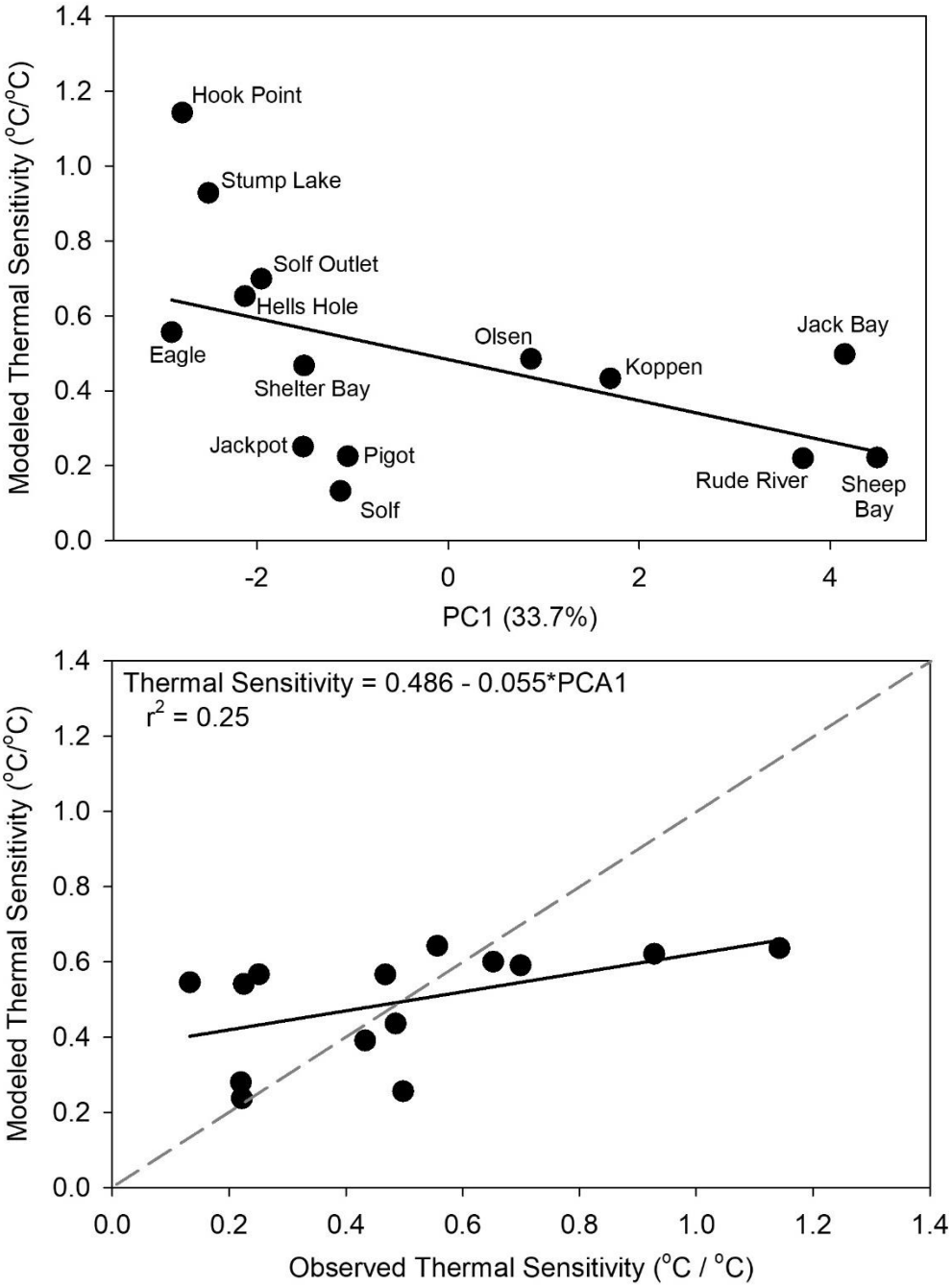

We further examined a subset of variables with high loadings (negative or positive) on PC1 for their direct influence on observed thermal sensitivity (Figure 11A-D). Relationships with individual variables tend to be weak. Clearly, our data include only a few large watersheds. While the largest watersheds did have low thermal sensitivity, so too did at least some watersheds across the full range of sizes we sampled. Both elevation and mean temperature appear to be more strongly related to thermal sensitivity, with stream temperatures in watersheds that have higher mean elevation and lower mean annual air temperature being less sensitive to increases in air temperature. Similarly, the few watersheds with a substantial proportion of area in perennial ice and snow also had low thermal sensitivity.

**Figure 11A-D:** Relationship between individual predictor variables with high loadings on PC1 and the observed thermal sensitivity among the 14 study sites in Prince William Sound.

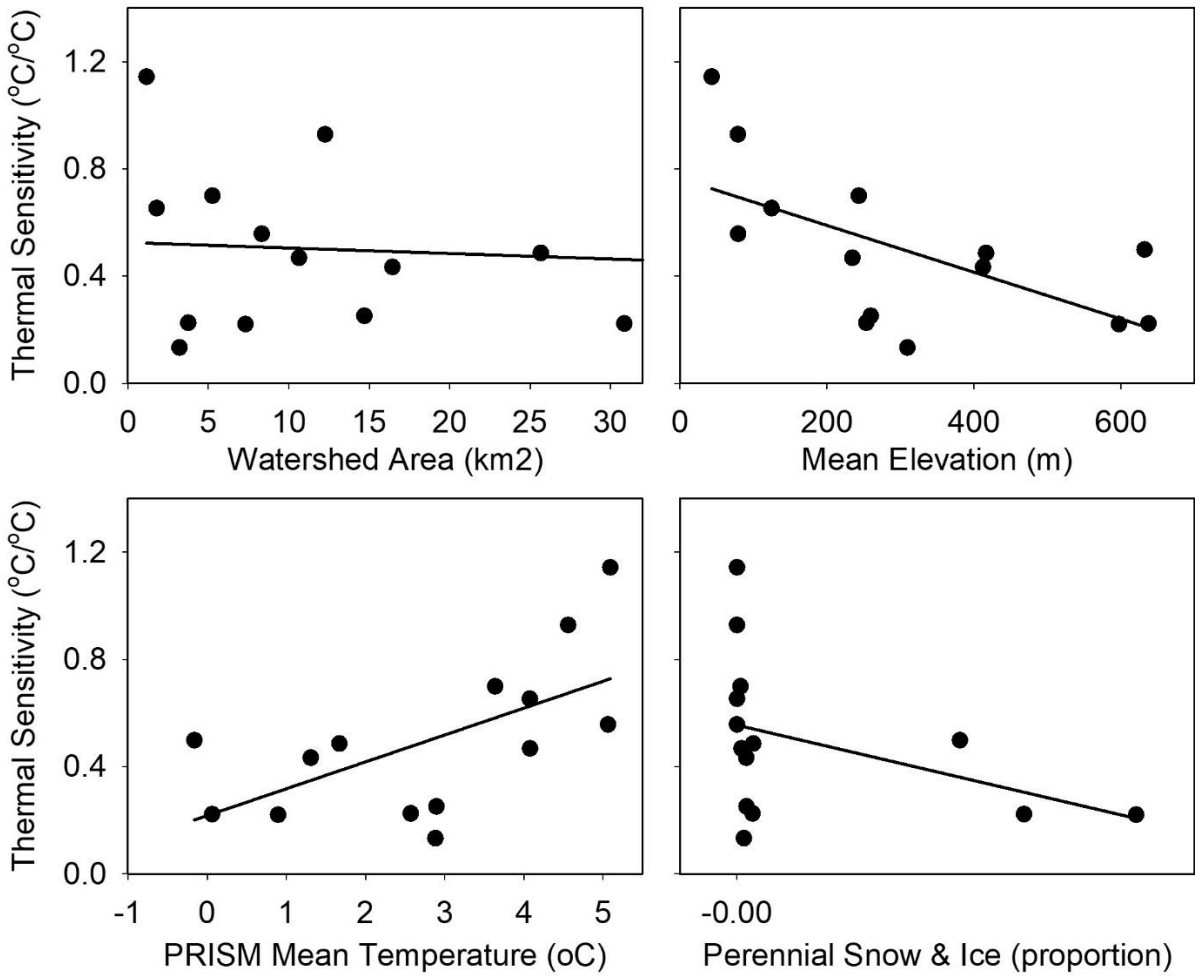

Given the relatively poor performance of PC1 to predict the observed thermal sensitivity, we turned to multiple linear regression in an attempt to relate the landscape variables to the thermal metrics. We first used a stepwise variable selection to objectively identify the best predictor variables. We used a significance level of 0.15 for variables to both enter the model and stay in the model in subsequent steps; variable selection ended when no additional variables could either be added or removed from the model. The model results were better, with the slope of the regression between the observed and predicted thermal sensitivity much closer to 1.0 and an $r^2$ of 0.64 (Figure 12). However, some variables included in the model appear spurious (Figure 13A-D). For example, we see no reason that the proportion of the watershed in coniferous forest would influence thermal sensitivity of stream water over the incubation period when that area ranges from 0% to only 6% and when shade should have little effect on stream temperatures. Similarly, we do not have a mechanistic explanation for why the proportion of the watershed that had either volcanic, sedimentary, or a combination of these parent materials would be related to thermal sensitivity. We have very uneven distribution of watersheds with high relative areas of either wetlands or lakes and ponds, however, their presence is clearly related to high thermal sensitivity among the watersheds we sampled (Figure 13A-D).

**Figure 12:** Stepwise multiple linear regression fit between observed thermal sensitivity and the sensitivity predicted from the regression model.

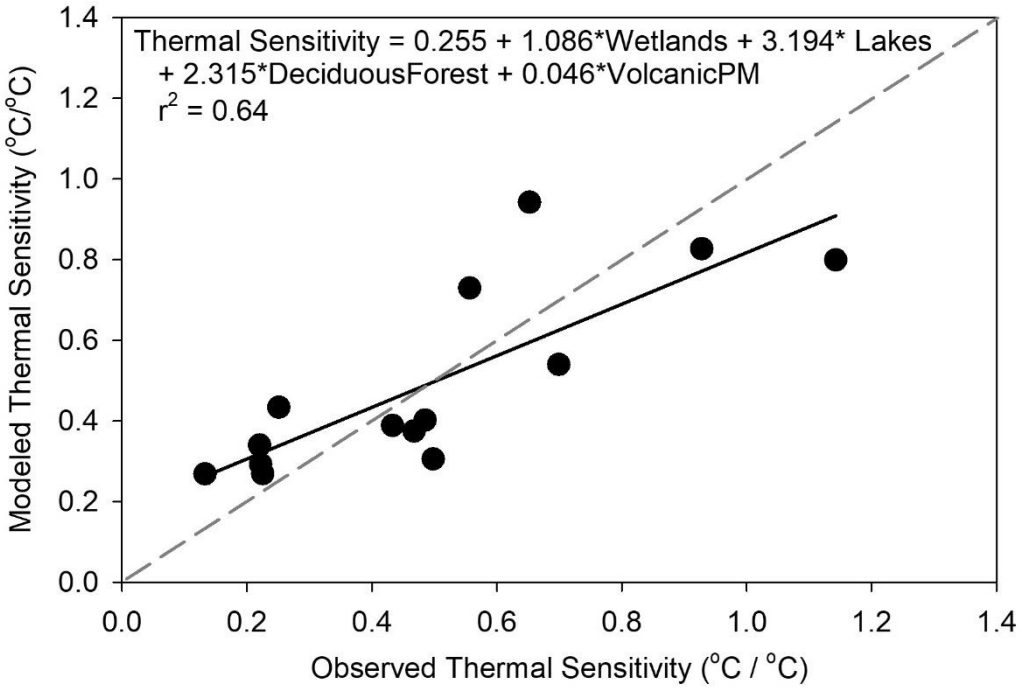

**Figure 13A-D:** Relationship between individual predictor variables selected in the stepwise multiple linear regression and the observed thermal sensitivity among the 14 study sites in Prince William Sound.

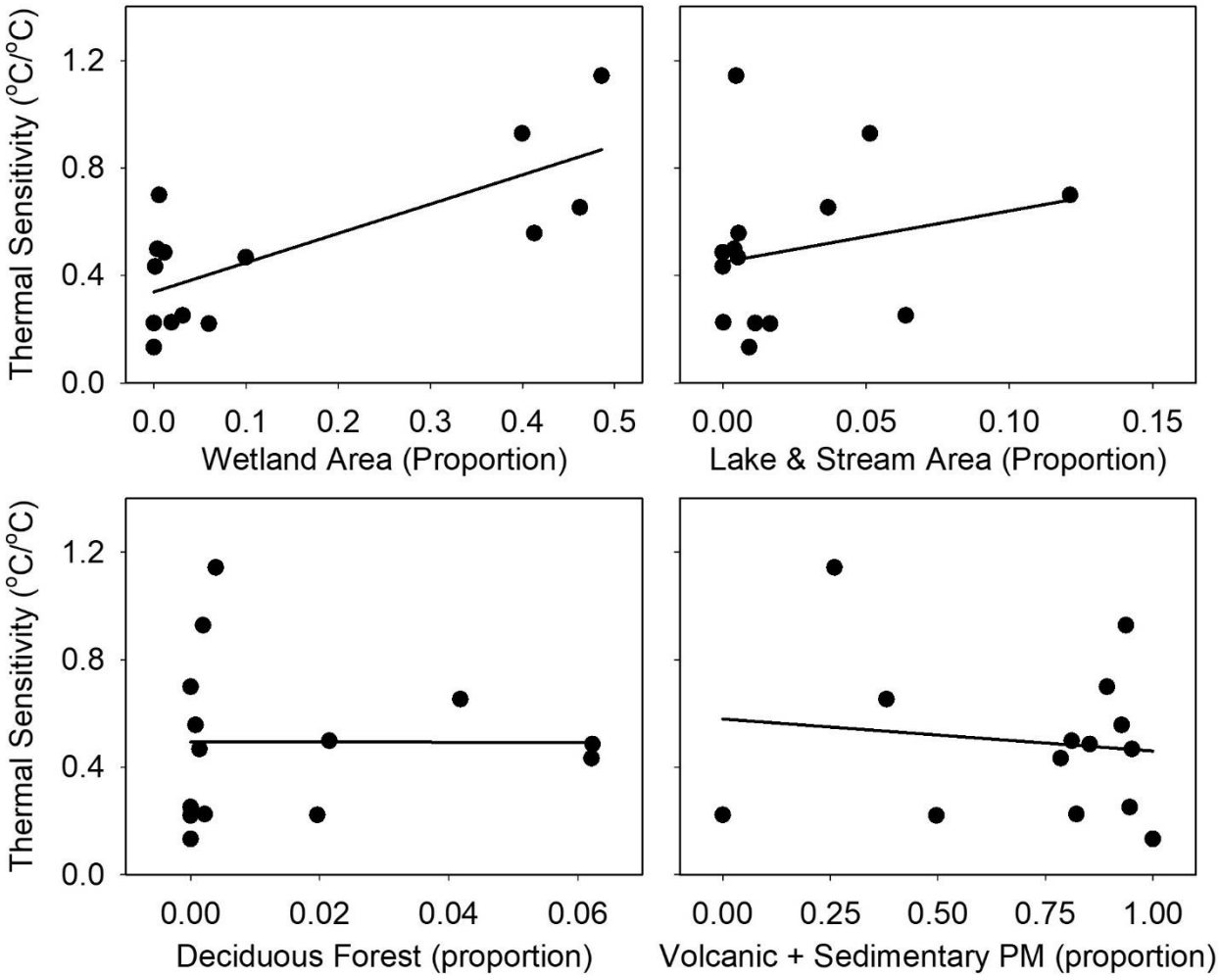


Finally, given the relatively poor performance of PC1 to predict the observed thermal sensitivity, and the high number of apparently spurious variables included through the stepwise regression procedure, we selected a handful of variables for which we could hypothesize a mechanistic relationship. We selected only from those variables that either showed high loadings on PC1 or were included in the stepwise model selection. We used these variables in a multiple linear regression to predict the observed thermal sensitivity. Overall, the model performed well with an $r^2$ of 0.69 without any variables that we had previously identified as generating likely spurious relationships (Figure 14).

**Figure 14:** Fit between observed thermal sensitivity and a multiple linear regression model parameterized with user-selected variables.

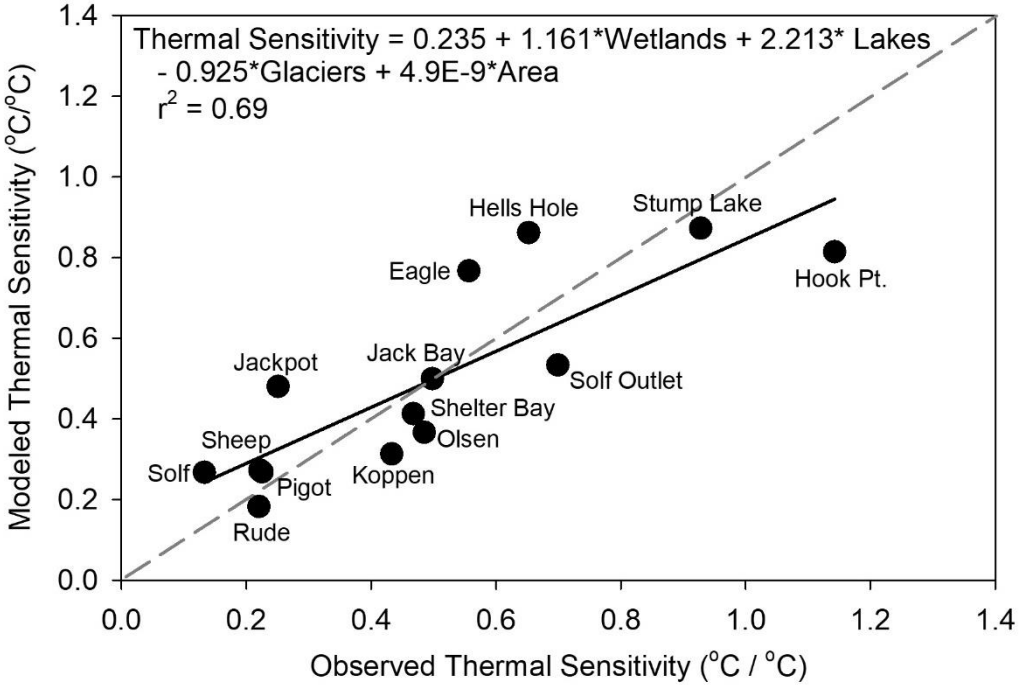


The model is reasonably parsimonious, however, several variables make relatively small contributions to the overall model fit as judged by the incremental increase in the cumulative $r^2$ as each new parameter is added to the model, and the parameter significance judged by the probability of a greater t-value in the final model (Table 6).

**Table 6:** Fit between observed thermal sensitivity and a multiple linear regression model parameterized with user-selected variables.

| Parameter | Final Estimate | Cumulative $r^2$ | Final P > t |
|---|---|---|---|
| Intercept | 0.235 | | 0.059 |
| Wetlands | 1.161 | 0.554 | 0.004 |
| Lakes & Ponds | 2.213 | 0.609 | 0.202 |
| Glaciers | -0.925 | 0.658 | 0.324 |
| WS Area | 0.000 | 0.695 | 0.174 |

We conducted similar analyses to find the best landscape predictor variables to project estimated thermal sensitivities derived from the best-fit regression models. We used those regression models and predicted the change in water temperature that might occur from a 4 °C increase in air temperatures. The language describing the results of the multiple linear regressions can be a bit confusing because we are now using a "predicted thermal sensitivity" and attempt to model that sensitivity using landscape predictor variables which then results in a landscape model for the "predicted thermal sensitivity" across the watersheds of Prince William Sound. We refer to these as the "Actual Predicted" and the "Model Predicted" thermal sensitivities on the x- and y-axes of the following graph (Figures 15).

As with the previous analyses, the multiple linear regressions identify a small number of landscape variables that provide high explanatory power within our dataset. These include either, or both variables for the proportion of the watershed area with wetlands or open water (Figures 15). These results satisfy expected mechanistic relationships, in which large areas of open water are exposed to solar radiation during the long, sub-arctic summer days leading to very warm summer temperatures. Also, ice that formed on the lakes and in the wetlands must melt in the spring before water begins to warm. However, average winter temperatures are close to freezing and during recent warm winters, ice cover has been thin and transient in low elevation watersheds in Prince William Sound and on the Copper River Delta. Loss of ice cover in the winter or early in the spring also leads to increased thermal sensitivity.

The stepwise variable selection procedure also includes landscape predictor variables in the regression model for which mechanistic relationships are unclear. These may result from spurious relationships and thus not be indicative of any mechanistic process. It is also possible that the underlying correlation structure within our dataset may allow the regression model to include a variety of effects from other variables that are not, themselves, selected for the model. At any rate, we do not currently have good mechanistic explanations for why PRISM minimum watershed temperatures might be related to the thermal sensitivity of the stream water to changes in air temperature (Figures 15).

**Figure 15: A)** Comparison among thermal sensitivity predicted by the model with the best NSC objective function and the stepwise multiple linear regression, **B-D)** relationship between individual predictor variables and the thermal sensitivity.

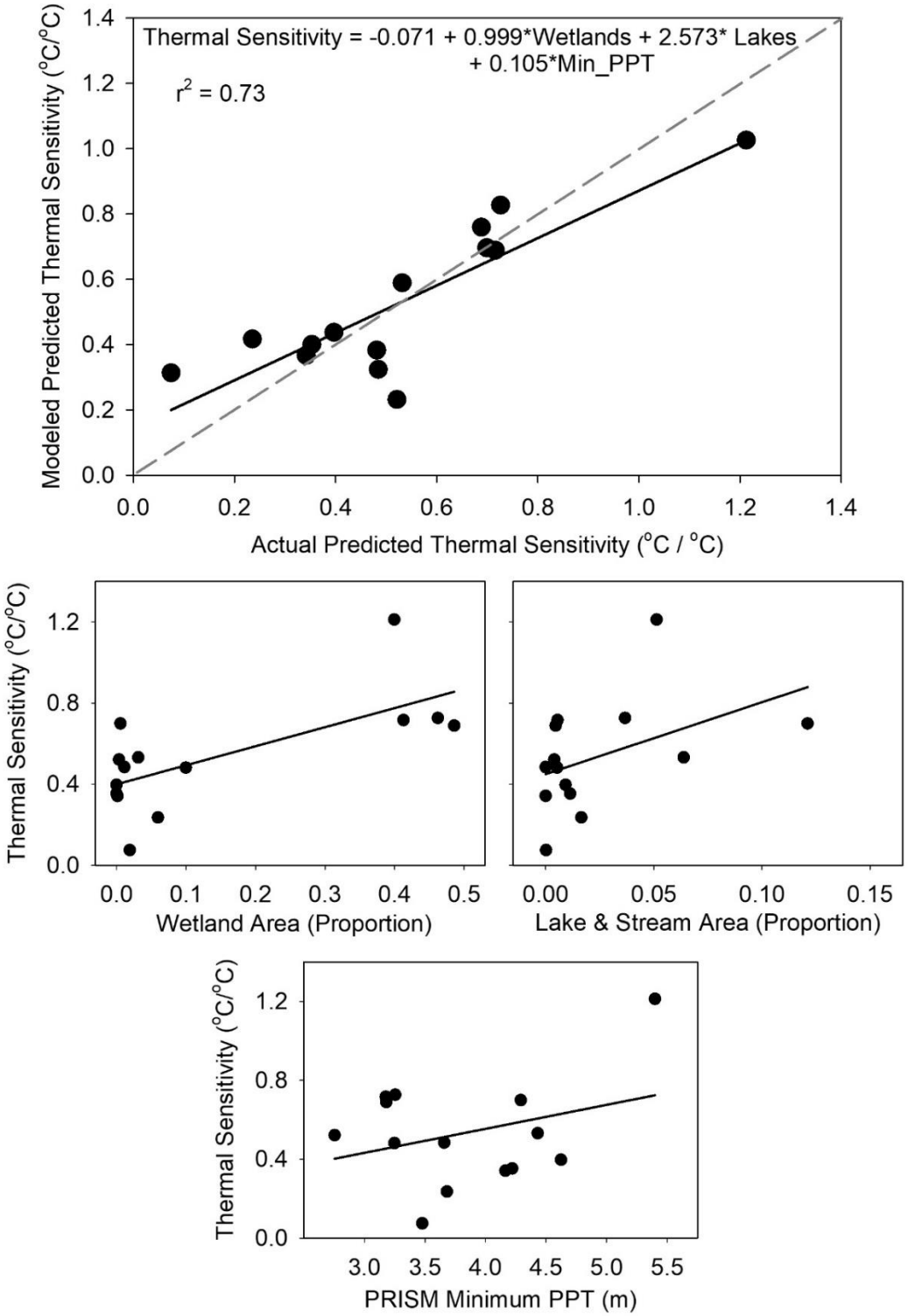

Finally, despite substantial effort to generate different (and potentially independent) measures of thermal sensitivity, our measures of thermal sensitivity over the incubation period were themselves correlated. Thus, models that had high explanatory power for one measure of thermal sensitivity often worked well for other measures. Compare for example, the model with user-selected variables for the observed thermal sensitivity between WY2016 and WY2017 (Figure 14) with the predicted sensitivity from the models that provided the best fit to mean daily air temperatures (the NSC objective function; Figures 15 and 16).

**Figure 16:** Fit between the actual predicted thermal sensitivity from the models that provided the best fit to mean daily air temperatures (the NSC objective function) and the modeled thermal sensitivity using a multiple linear regression model parameterized with user-selected landscape predictor variables.

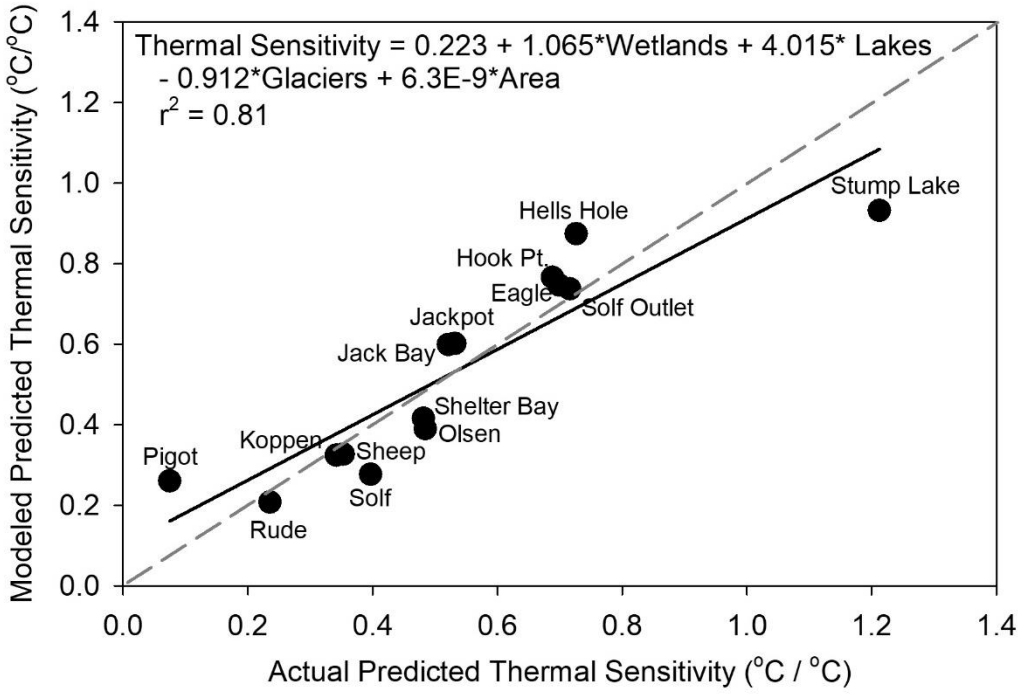

**Projecting Thermal Sensitivity across Prince William Sound:**

We used the predictive models described above (Figures 14 & 16) to project thermal sensitivities for Hydrologic Unit Code 6 (HUC6) watersheds of Prince William Sound (Figures 17 and 18). Where HUC boundaries are coincident with the land-ocean interface, the HUC usually includes many smaller, disconnected watersheds, each with its own outlet to the ocean. Thus, the landscape predictor models developed for discrete watersheds give only a general potential thermal sensitivity for all watersheds within each HUC. Individual watersheds might have very different thermal sensitivities.

**Figure 17:** Project thermal sensitivities for Hydrologic Unit Code 6 (HUC6) watersheds of Prince William Sound based on observed stream water sensitivities to changes in observed air temperatures between the water years 2016 (warm) and 2017 (cold).

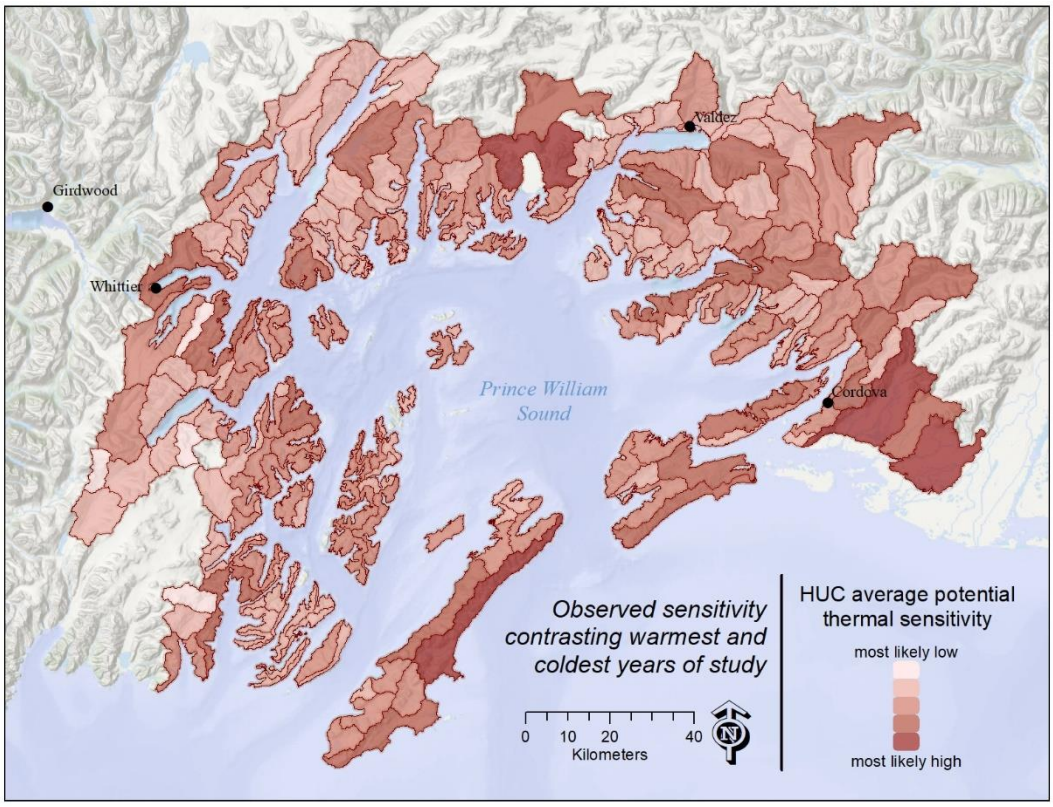

**Figure 18:** Project thermal sensitivities for Hydrologic Unit Code 6 (HUC6) watersheds of Prince William Sound based on thermal sensitivities predicted from best fit models using the NSC objective function and a 4° C increase in air temperature.

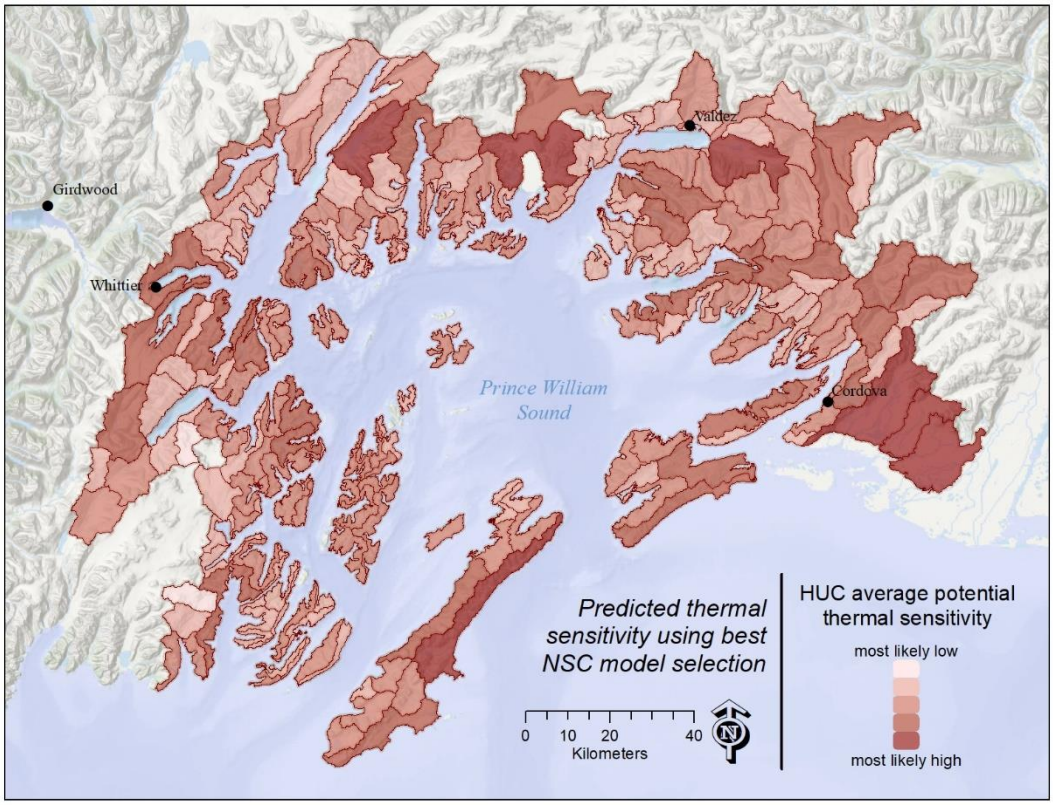

**Potential impacts of climate change on water temperature:**

We used the air-water regression models to obtain an estimate of potential climate change impacts to water temperature at our study sites. To perform this analysis, we calculated day-of-year average temperatures, effectively a four-year daily average, for all 365 days of the calendar year (29 February was excluded) using four time series of mean daily data: Observed, Modeled, Scenario 1, and Scenario 2.

The observed time series was generated from the daily mean water temperature data we collected at each site during the entire study period. The modeled time series was generated from air temperatures during the study period using the "best" air-water temperature regression model fitted for each site, as described in the Thermal Sensitivity section. Scenarios 1 and 2 were also generated using the best regression model for each site, however, we raised the input air temperature data by 4 °C as compared to the study period air temperature, representing a potential future climate scenario.

Although the same air temperature data were used at each site for Scenario 1 and 2, different coefficients were used to calculate water temperature during spring and early summer to represent two different snow melt scenarios. Scenario 1 used two sets of coefficients, one fitted to the seasonal meltwater hysteresis observed during the study period and one fitted to autumn cooling temperature limb when thermal sensitivity was higher. By accounting for seasonal meltwater hysteresis, the Scenario 1 model generated lower water temperatures in the spring than in the autumn at the same air temperature. The Scenario 2 model used only the coefficients fitted to the autumn cooling limb for each site, approximating a scenario where meltwater hysteresis was absent. This model simulated a rain-dominated precipitation regime, a state that is anticipated to be increasingly present at lower elevations and sites more proximate to the Gulf of Alaska with climate change. We calculated the differences between each of the future Scenarios and the modeled day-of-year average temperature for each site in order to identify times of year with the most and least water temperature response to future climate warming.

Observed and modeled temperatures were similar, indicating good regression model fit (Table 7. and Figure 19). Day-of-year mean water temperature was elevated by up to 7.4 °C under PC4 1, the warming−snow scenario. The average change across all sites was 2 °C, indicating the average stream warmed half as much as the air temperature. On 25% of days, the water temperature change was less than 1 degree under Scenario 1. We projected greater warming under Scenario 2, the warming−no snow scenario. The combination of 4 °C warmer air temperature and no meltwater hysteresis resulted in an average water temperature increase of 2.6 °C and a maximum increase of more than 10 °C as compared to modeled day-of-year water temperatures during the study period.

**Table 7**. Day-of-year temperature statistics calculated from air temperature and four water temperature data sets: Observed, Modeled, Scenario 1(S1), and Scenario 2 (S2).

| **n=5,110** | **Temperature Data Types (°C)** | | | | | | |
|---|---|---|---|---|---|---|---|
| | **Air** | **Observed** | **Modeled** | **S1 (snow)** | **S2 (no snow)** | **Difference S1 – Modeled** | **Difference S2 – Modeled** |

| | | | | | | | |
|---|---|---|---|---|---|---|---|
| **Min** | -7.8 | 0.1 | 0.2 | 0.5 | 1.2 | +0.0 | +0.1 |
| **25%** | 0.0 | 2.0 | 2.3 | 4.1 | 4.8 | +1.0 | +1.4 |
| **Median** | 4.2 | 4.2 | 4.2 | 0.5 | 7.3 | +1.7 | +2.4 |
| **50%** | 5.0 | 5.3 | 5.3 | 7.4 | 8.0 | +2.0 | +2.6 |
| **75%** | 10.6 | 7.9 | 7.8 | 9.6 | 9.7 | +2.7 | +3.6 |
| **Max** | 15.6 | 19.1 | 19.0 | 23.3 | 23.3 | +7.4 | +10.1 |

**Figure 19**. Day-of-year water temperatures for the study sites generated from observed (black), modeled (gray), Scenario 1 (blue), and Scenario 2 (orange) data.

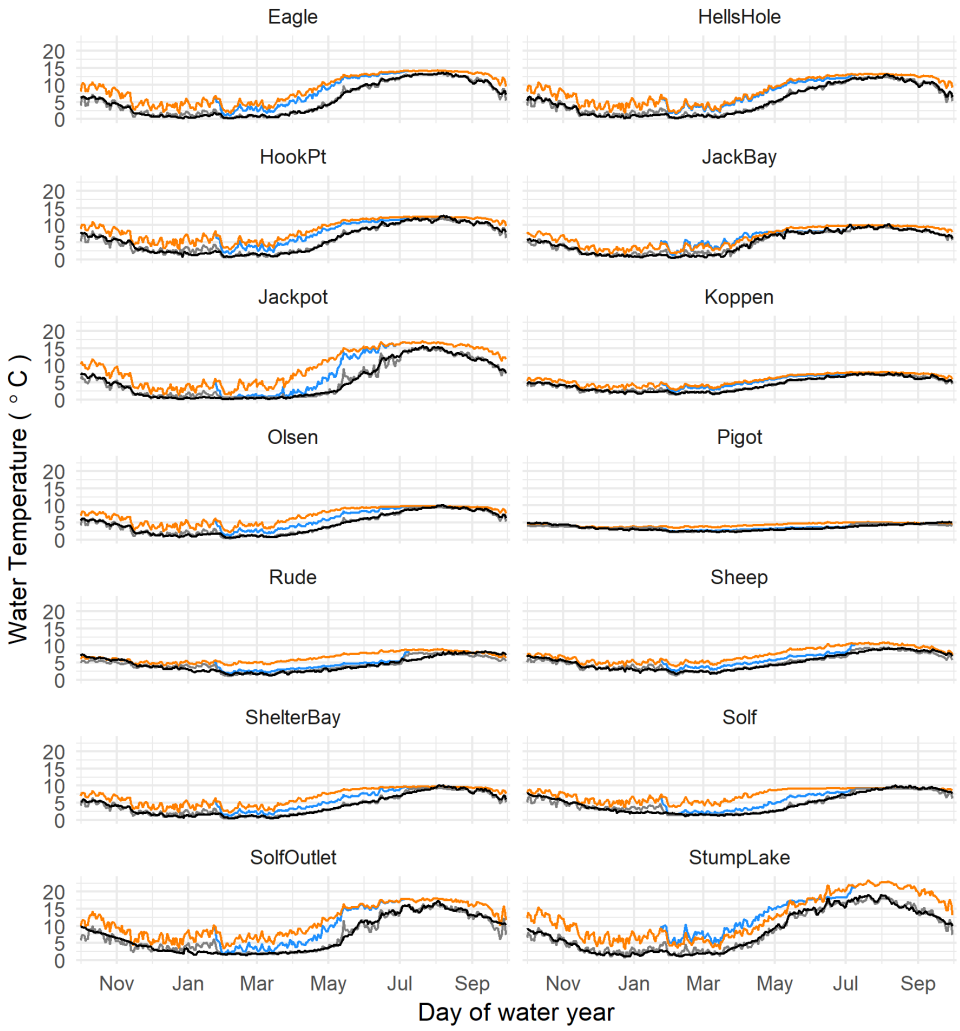


**Potential impacts of climate change on duration of egg incubation:**

To better anticipate potential climate change impacts on the duration of incubation for Coho Salmon eggs, we modeled incubation during the study period and under the two warming

scenarios described above. We calculated duration of incubation with an empirically-derived Bělehrádek model (Alderdice and Velsen 1978) that was developed by Beacham and Murray (1990) and modified by Sparks et al. (2018). Beacham and Murray fitted 10 models to development data collected for Coho Salmon embryos, and determined the log-inverse Bělehrádek model was among the best-fitting models ($r^2 = 0.98$) across a range of mean incubation temperatures (1.5 to 12°C). Sparks et al. modified the Beacham and Murray approach by solving for the inverse of the original function, which they described as the daily "effective value." The effective value model equation is:

Eq. 1

$$E_i = \frac{1}{\exp\left(7.018 - 1.069 * \log_e(T_i + 2.062)\right)}$$

where $E_i$ is the relative daily effective value, which has a range of 0–1, and $T_i$ is the day-of-year mean water temperature (°C) selected from one of the four data time series described in the last section: Observed, Modeled, Scenario 1, and Scenario 2.

We calculated the duration of incubation for early, mid, and late spawning Coho Salmon by counting from the assumed spawn date until the date fry emerge from the gravel (when E=1), as predicted by the effective value model. Based on our observations of spawning adult salmon in the study area, we estimated an early spawn date of September 15$^{th}$, a middle spawn date of October 15$^{th}$, and a late spawn date of November 15$^{th}$. Spawn date almost certainly varied by stream and water temperature regime during the study period, but here we applied all three dates to all sites because Coho Salmon are likely to adapt spawn timing in the future in response to changing environmental conditions (Crozier et al. 2008). We applied a Welch two-sample *t*-test to test the hypothesis that the duration of incubation was the same during the study period and each future scenario.

The mean duration of incubation calculated with observed and modeled day-of-year water temperatures varied by less than 12 days across all the sites, indicating good model fit during the study period (Figure 20). Interestingly, the mean duration of incubation calculated from modeled temperatures was nearly identical for eggs laid by mid and late spawning fish. Duration of incubation was two to three weeks shorter for eggs laid by early spawning fish (Table 8).

**Figure 20.** Duration of incubation at each study site modeled from observed, modeled, Scenario 1 (warming−snow), and Scenario 2 (warming−no snow) day-of-year mean water temperatures using a spawn date of September 15 (top), October 15 (middle), and November 15 (bottom).

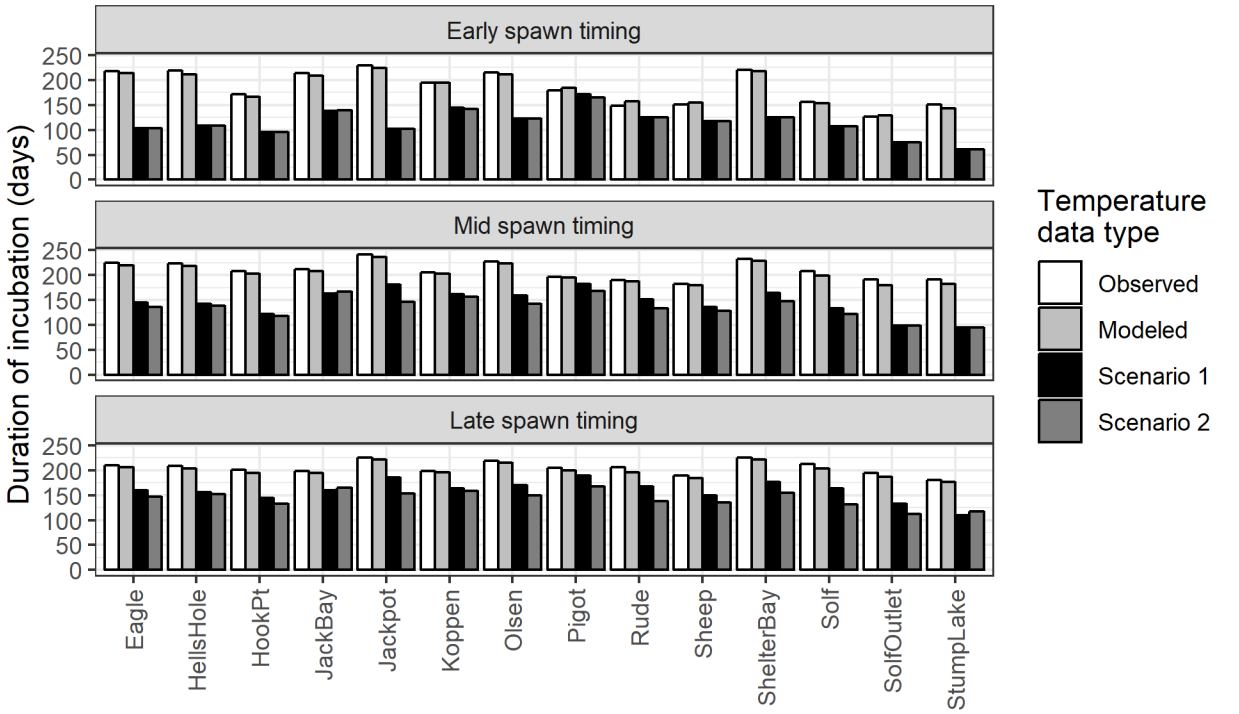


**Table 8.** Mean incubation duration and temperature, and mean emergence date calculated from four day-of-year temperature data series (Observed, Modeled, Scenario 1, and Scenario 2) for three spawning periods at all the study sites.

| Spawn Timing | Data Type | Mean incubation duration (days) | Mean temperature (°C) | Mean emergence date |
|---|---|---|---|---|
| Early (Sept. 15) | Observed | 185 | 3.4 | 3/18/2017 |
| | Modeled | 184 | 3.4 | 3/16/2017 |
| | Scenario 1 | 114 | 6.8 | 1/6/2017 |
| | Scenario 2 | 114 | 6.8 | 1/5/2017 |
| Mid (Oct. 15) | Observed | 210 | 2.7 | 5/11/2017 |
| | Modeled | 205 | 2.8 | 5/6/2017 |
| | Scenario 1 | 145 | 4.9 | 3/8/2017 |
| | Scenario 2 | 136 | 5.3 | 2/26/2017 |
| Late (Nov. 15) | Observed | 206 | 2.8 | 6/7/2017 |
| | Modeled | 200 | 2.9 | 6/1/2017 |
| | Scenario 1 | 159 | 4.2 | 4/22/2017 |
| | Scenario 2 | 144 | 4.8 | 4/7/2017 |

The future warming scenarios corresponded with a significant ($t > 6.2$, $df = 23$, $p < 0.00001$) reduction in duration of incubation (Figure 21). The mean duration of incubation was 57 days shorter under Scenario 1, the warming−snow scenario, as compared to the study period. The eggs of early spawning fish were most affected (a 70 day reduction) while eggs of late spawning fish were least affected (a 41 day reduction), indicating that for Scenarios 1 and 2 water temperatures warmed more in late September and early October than March or April.

Springtime warming was greater under Scenario 2, the warming− no snow scenario, when the mean duration of incubation was reduced by 65 days as compared to the study period. Duration of incubation was nearly identical under the 2 scenarios for the eggs of early spawning fish because alevin were projected to emerge from the gravel during the winter, before melting occurred under the Scenario 1. The offspring of mid spawning fish typically emerged earlier under the Scenario 2 as compared to the Scenario 1, but the difference was not significant ($p = 0.31$). For the offspring of late spawning fish, duration of incubation was significantly ($t=2.2$, $df=25$, $p=0.04$) reduced under Scenario 2 as compared to Scenario 1. The greatest difference was observed at Jackpot Lake, a cold and snowy site that was high in elevation, where emergence was up to one month earlier under Scenario 2.

**Figure 21**. Dots represent duration of incubation at each site generated from observed, modeled, Scenario 1 (warming−snow), and Scenario 2 (warming−no snow) day-of-year mean water temperatures for the eggs of early (September 15), mid (October 15), and late (November 15) spawning salmon. Bars represent the mean for each group.

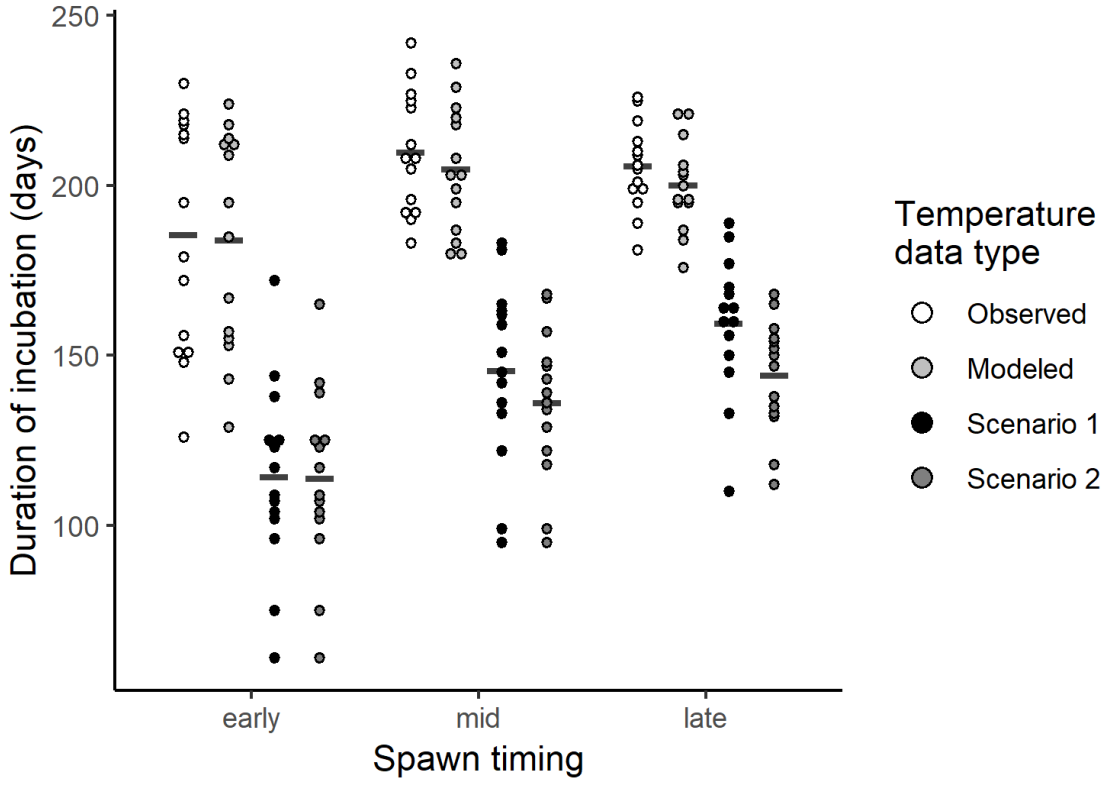

**Analysis of potential future maximum temperatures**:

For Alaska's warmest watersheds, maximum summer temperatures may become increasingly seasonally unfavorable for cold-water fish (including salmonids) with increasing climate warming, a habitat feature that is already common for many salmon watersheds at lower latitudes. As long as fish within a population have habitat options for carrying out their life history (spawning, incubation, rearing, migration to and from the ocean), movement between favorable habitats (and away from unfavorable habitats) can allow for productive populations.

We used the regression equations relating mean weekly air temperature to mean weekly stream temperature to project daily time series of stream temperatures under a warmer climate when air temperatures were 4° C warmer than observed during our study. We calculated the 7 day running average of the daily average (7DADA) from these time series and then used multiple-linear regression to relate projected future 7DADA to watershed characteristics. Perhaps not surprisingly, the proportion of the watershed area in lakes and ponds and the proportion of watershed area in wetlands were reasonably good predictors (Figure 22), although our landscape model substantially under-predicted the temperature of our warmest site, Stump Lake. Clearly, despite frequently overcast days, occasional cloud-free days combined with indirect solar radiation during the long, sub-arctic summer days substantially warmed exposed water – especially in large shallow lakes leading to high summer time maximum temperatures.

Sites at three of our studied watersheds had surprisingly high 7DADA during the 4-year study. We followed Mantua et al. (2010) who used 21° C as a critical weekly average temperature threshold for thermal migration barriers for salmonids in Washington State. One site, Stump Lake, already exceeds this temperature and the 7DADA is expected to increase to 25° C under a warming climate. Two sites, Jackpot Lakes and Solf Lake Outlet had 7DADA in excess of 16° C and are expected to increase to 18° C in the future.

We used our landscape model from Figure 22 to project a likely response surface for future 7DADA (Figure 23). Among our study sites, the proportion of the watershed area in lakes ranged from 0% to 12% and wetlands ranged from 0% to 49%. Clearly, watersheds with large shallow lakes are likely to exceed the 21° C threshold in the future; the proportion of wetland area also contributes to future climatic vulnerability. There is substantial uncertainty in our model projections, with 7DADA for some sites either substantially under predicted or over predicted.

We used the predictive model (Figure 22) to project thermal sensitivities for Hydrologic Unit Code 6 (HUC6) watersheds of Prince William Sound (Figures 24). Where HUC boundaries are coincident with the land-ocean interface, the HUC usually includes many smaller, disconnected watersheds, each with its own outlet to the ocean. Thus, the landscape predictor models developed for discrete watersheds give only a general potential thermal sensitivity for all watersheds within each HUC. Individual watersheds might have very different thermal sensitivities.

**Figure 22: A)** Comparison between the landscape-based model of the maximum 7-Day Running-Average of the Daily Average temperature (7DADA) and the 7DADA predicted for the 14 study sites from the regression model with the best NSC objective function, **B-C)** relationship between individual predictor variables and the 7DADA.

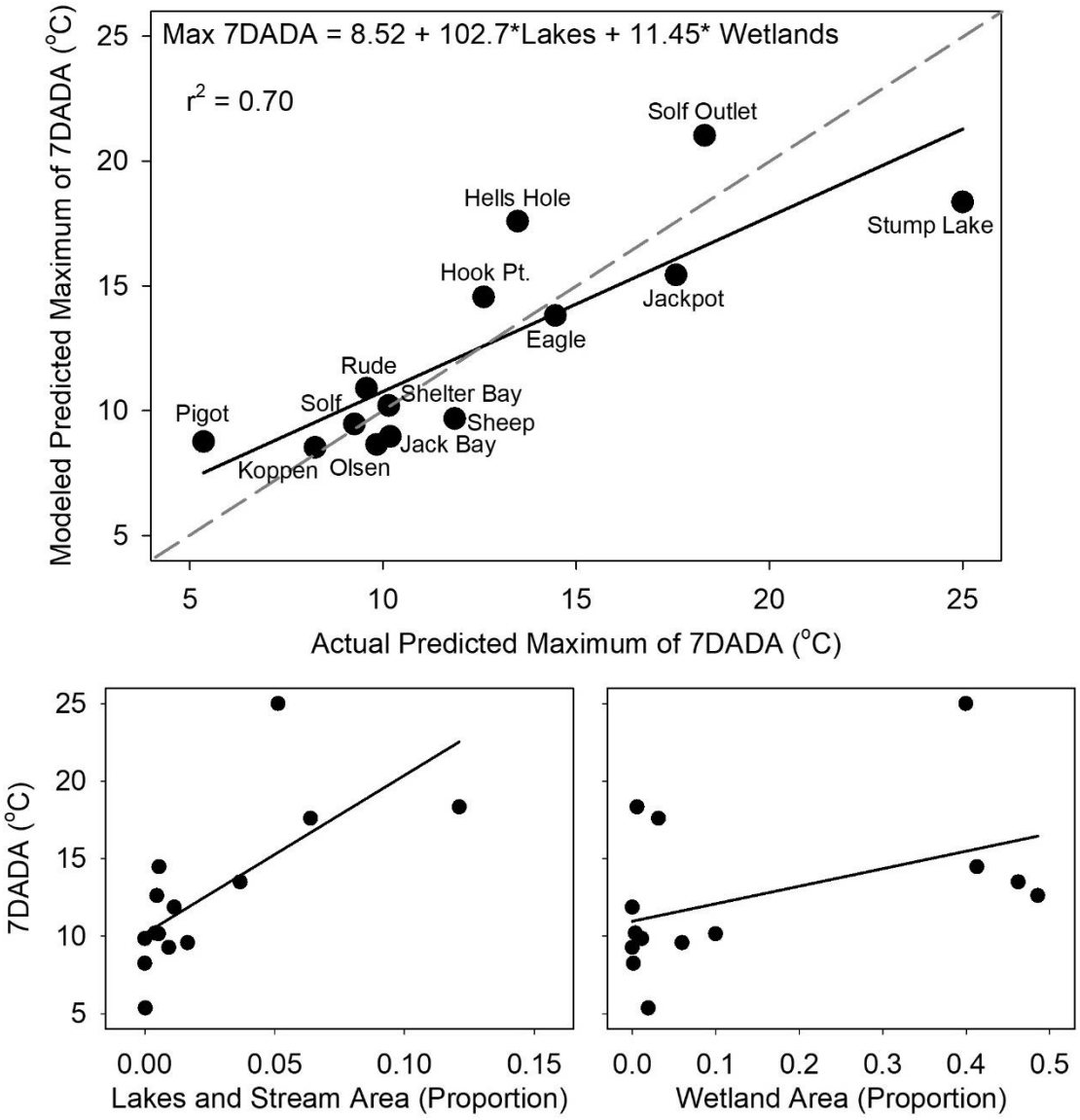

**Figure 23:** Response surface from the landscape model relating the proportional area of lakes (x-axis) and wetlands (y-axis) to the predicted future 7DADA (contours). The region exceeding the 21° C critical temperature threshold (Mantua et al., 2010) is shaded pink. The 14 study sites are overlaid on the response surface, based on the actual area of lakes and wetlands in each subtending watershed. The 8 sites with more than 1% lake area or 5% wetland area are identified and the actual projected future 7DADA is given (circled numbers) to illustrate how model uncertainty influences the ability to project climatic vulnerability to the larger landscape.

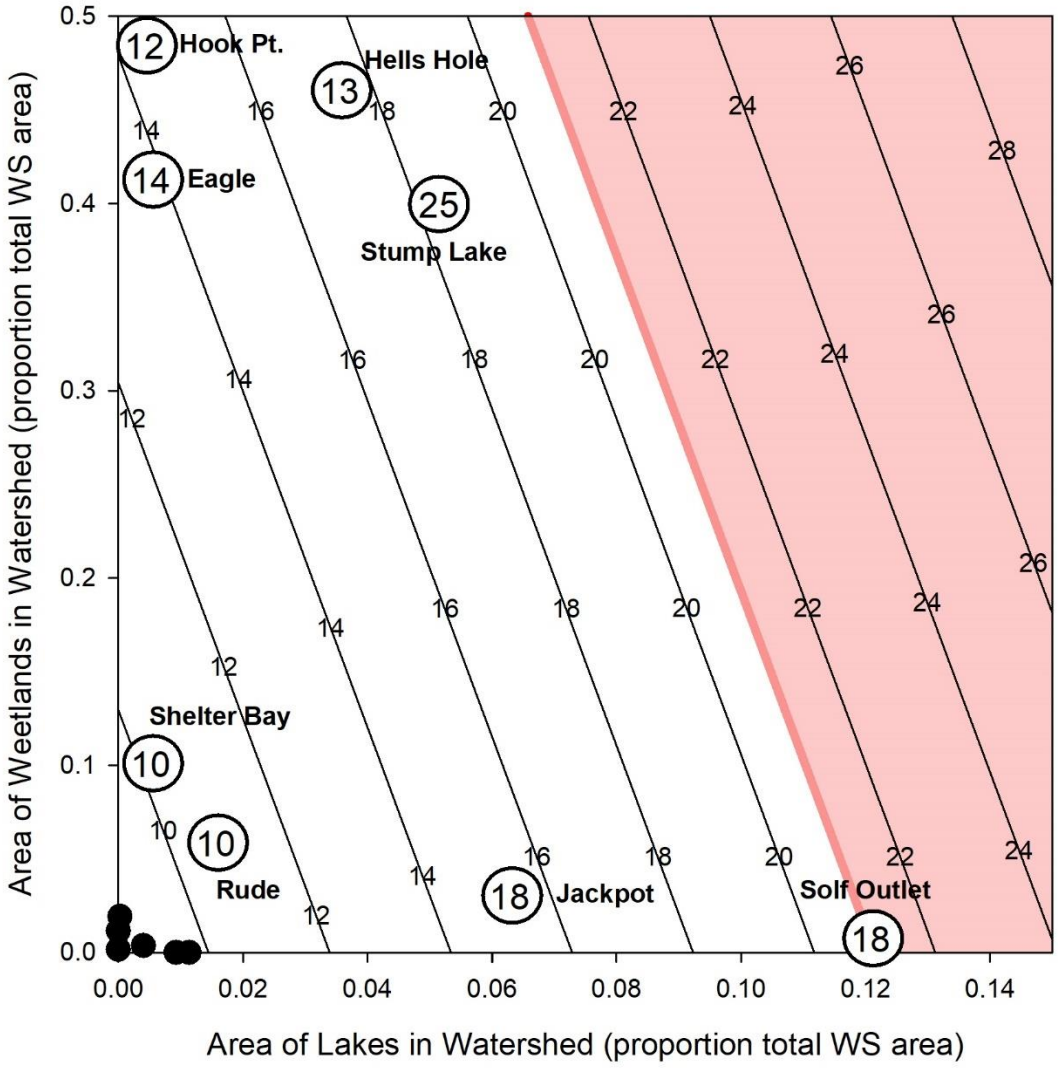

**Figure 24:** Project future maximum of the 7-day running average of the daily average temperature for Hydrologic Unit Code 6 (HUC6) watersheds of Prince William Sound under a 4° C increase in air temperature.

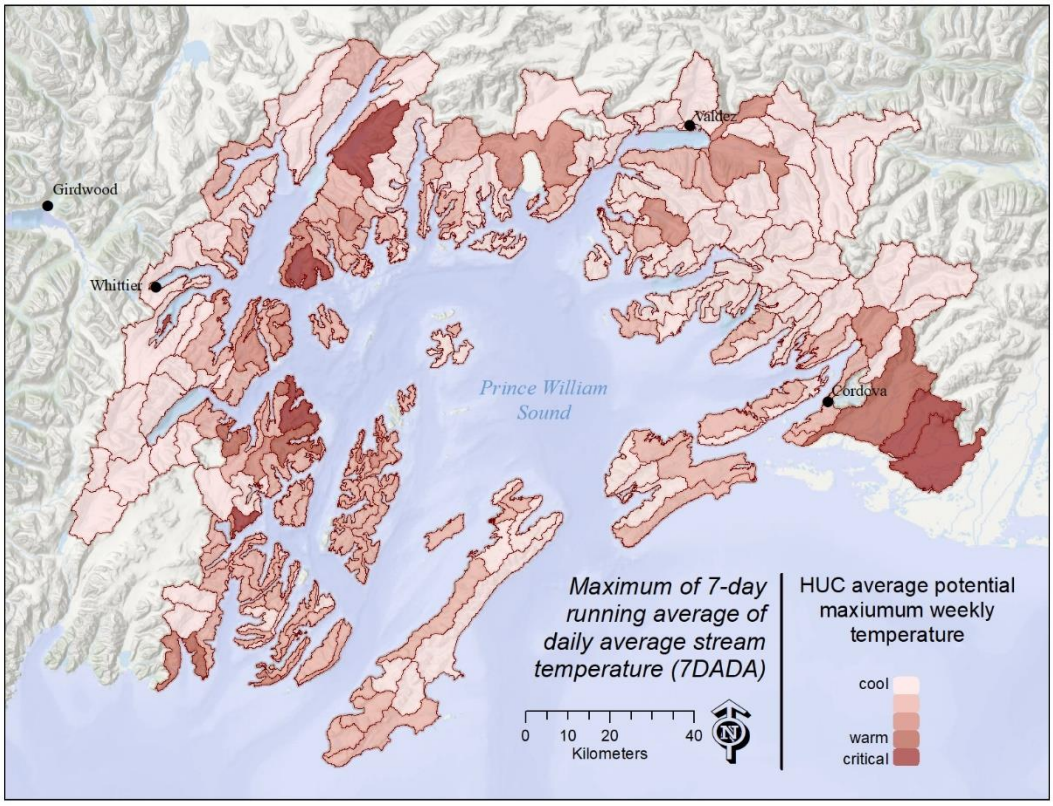

**Tidal Influence on Stream Temperatures:**

We observed unexpected temperature fluctuations at some of our study sites over the course of the study, with occasional increases in stream and streambed temperatures lasting many hours over a series of successive days over the winter incubation period (Figure 25A). The regularity of these warm-water pulses made us curious if they could result from intrusion of tidal waters during the highest, or spring tides. We compared tidal ranges in typical mean ocean temperatures over these periods and found that we only observed the abrupt changes in temperature on days with very high tides (exceeding 4.5 m at the Cordova AK tide gage) (Figure 25B). Further, the temperature spikes reached almost exactly the mean ocean temperature.

**Figure 25:** A) Bed-sediment water temperatures at the upper limit of the intertidal zone showing tidal influence (sharp vertical departures from the temperature trend) compared to mean daily ocean temperature from 2014 to 2018 (several months of missing ocean temperature data during the winter 2014-15 forced the use of a multi-year mean for comparison purposes). B) Maximum daily tidal height at Cordova, AK. Tides exceeding 4.5 m inundated the stream at the monitoring site leading to sharp rises in temperature. Note: the time periods graphed here were much warmer than historical averages because the "Blob" (2013 to 2016) resulted in much warmer than average ocean temperatures in the north-east Pacific Ocean.

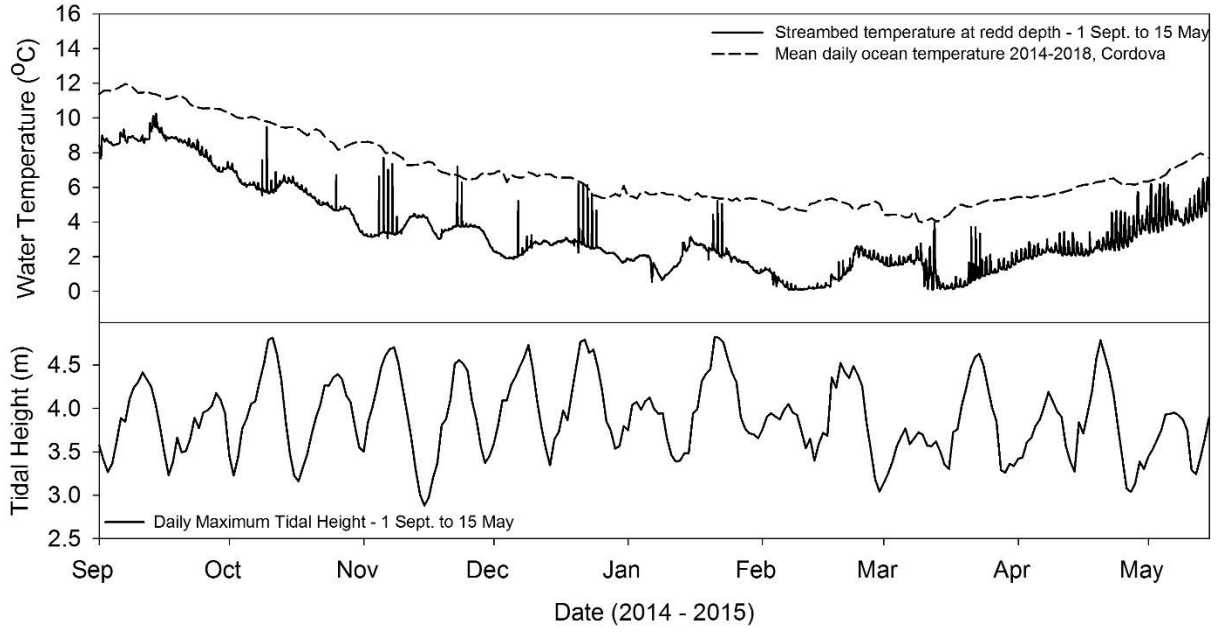


Pink and Chum Salmon spawn extensively within the intertidal zone which can provide a large proportion of the spawning habitat available throughout Prince William Sound and south-east Alaska where stream networks drain small watersheds in the steep coastal mountains. Low gradient reaches are limited to short distances from the ocean, beyond which stream gradients are typically too steep and bed sediment too coarse to support spawning. Also, upstream migration is often blocked by waterfalls a short distance from the ocean. Given these restrictions, the use of the intertidal zone may substantially increase the total amount of spawning habitat available. This is certainly true in the fiords of Prince William Sound where, in some streams, 45% (Thorsteinson et al., 1971) to as many as 75% of the Pink Salmon (Helle, 1970) and 90% of the Chum Salmon (Thorsteinson et al., 1971) spawn in the intertidal zone. Further, strong preference for the intertidal zone occurs even when freshwater spawning habitat is accessible and

uncrowded (Thorsteinson et al., 1971). Thus, our results raise the possibility that, over the incubation period, the thermal regimes in the lower reaches of streams used by spawning salmon in Prince William Sound may be influenced by the impacts of climate change on both ocean temperatures in the Gulf of Alaska and stream temperatures of the freshwater ecosystem.

The intertidal zone is a complex habitat with steep environmental gradients in both space and time that substantially influences the success of spawning salmon. Height above the low tide line (Mean Lower Low Water; MLLW) determines the duration of tidal inundation which in turn influences salinity, water temperature, and dissolved oxygen, and indirectly influences the amount of fine sediment in the streambed. The direct effects of salinity can be substantial. In a laboratory study that simulated tidal exposure to sea water salinity of 28 ppt, Bailey (1966) showed that 50% mortality of salmon embryos would occur if redds were inundated with salt water for 6 hours twice a day which would corresponding to two tidal cycles with a 2.1 m tidal height. Longer duration inundation increased mortality but saltwater exposure of 4 hours twice a day, corresponding to a 3.0 m tide, had no adverse effect. Using these data, and applying them to Olsen Ck. (Fig. 26), we would expect that salinities and inundation duration in the upper 525 m of the intertidal zone would have no effect on Pink Salmon embryos. Further, high embryo survival would be expected from 525 m to 750 m. Mortality would exceed 50% in the lowest reaches of the intertidal zone and in fact, little spawning activity is observed.

Given our preliminary results and the extensive use of the intertidal zone for spawning, we investigated the potential thermal sensitivity of the surface temperature of Prince William Sound using data recorded at the West Orca Bay Buoy (60.584 N 146.805 W; National Buoy Data Center, Station 4605050) in central-western Prince William Sound. During the summer, the ocean surface temperature appeared quite sensitive to air temperatures (Figure 27). In contrast, in winter, weekly-average ocean-surface temperatures never got colder than ~ 4 °C during the period of study and when air temperatures were below ~5 °C, the ocean surface temperature was uniform over time, suggesting that, during the winter, surface ocean temperatures are decoupled from air temperature. Two factors likely account for these differences. First, the relatively high sensitivity of air temperature during the summer appears to result from a stratified ocean, with the surface water heavily influenced by freshwater runoff from snow and ice melt (see Figure 28 from Campbell 2018). This lens of fresher water floats at the surface of PWS and due to stratification, it can heat without mixing with deeper, colder and saltier ocean water. This freshwater lens disappears in winter because cold temperatures stop snow and glacier melt. Without stratification, the depth of the mixing layer increases markedly, from only a few meters in summer to greater than 50 m by late winter (Campbell, 2018). The increase in mixing depth provides a large thermal reservoir that strongly damps changes in water temperature that might occur at the surface. Thus, ocean temperatures stabilize around 4 or 5 °C and by late winter, both temperature and salinity are relatively uniform over depth (see Figure 28 from Campbell 2019).

**Figure 26**: Depiction of the intertidal zone of Olsen Creek. The longitudinal gradient of the creek averaged over both pre- and post-1964 earthquake surveys was 0.399% (Thorsteinson et al., 1971, Table 3, pg. 206) which corresponds to a channel distance of 1275 m from the elevation of the annual highest tide (4.95 m) to mean lower low water (MLLW; 0.00 m). Tidal heights and the percent of the incubation period (1 Sept to 15 May) over which any given elevation is inundated by sea water were calculated from Cordova AK tidal predictions corrected for the average of the high- and low-tide offsets at Comfort Cove, Port Gravina. Embryo survival plotted on to the channel distances that would be inundated by sea water for the percentage of the incubation period corresponding to the inundation durations and survivals determined in a laboratory-simulated tidal environment

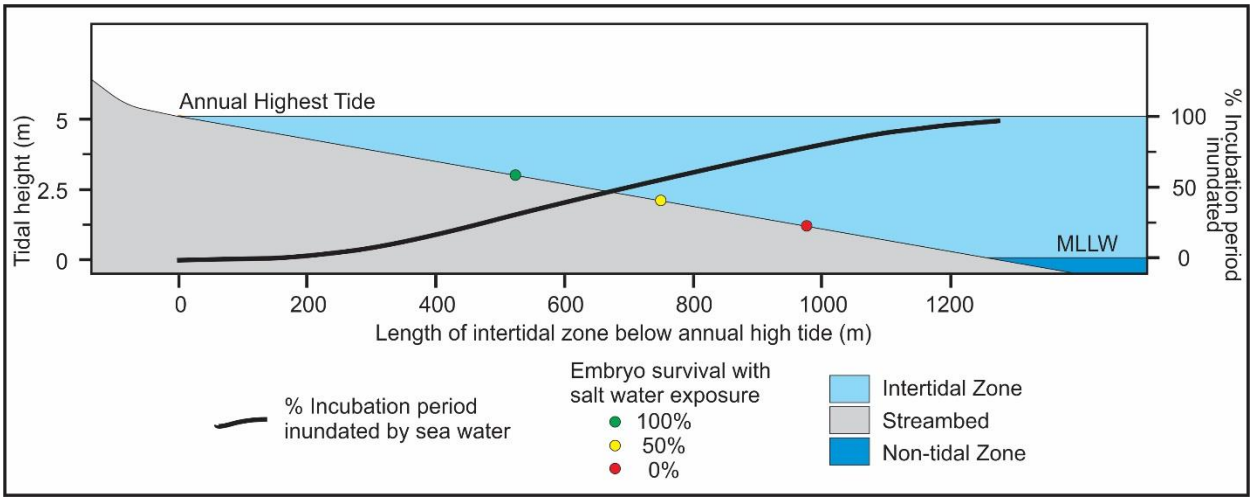


It is beyond the scope of this project to explore how ocean temperatures in the Gulf of Alaska, and in Prince William Sound in particular, will respond to climate change. However, these preliminary results strongly suggest that the incubation environment to which salmon respond is highly complex and future changes in that environment caused by a changing climate will respond to both effects within the terrestrial watershed and freshwater ecosystem and well as the Pacific Ocean.

**Figure 27:** Relationship between air temperature and ocean temperature measured at the West Orca Bay Buoy. Air temperatures are recorded 4 m above the ocean surface; ocean temperatures are measured 0.6 m below the ocean surface. (National Data Buoy Center https://www.ndbc.noaa.gov/station_page.php?station=46060&uom=M&tz=STN, Station 46060 located at 60.584 N 146.805 W (60°35'1" N 146°48'19" W, data downloaded on 19 Feb, 2019).

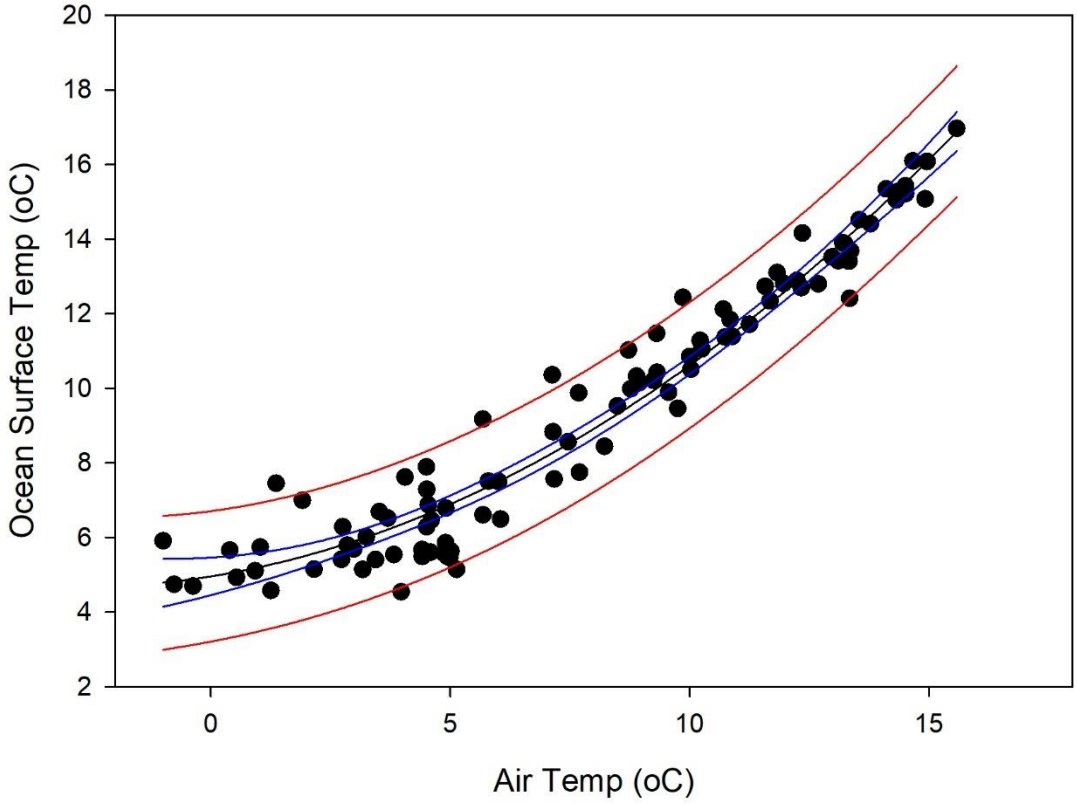

**Figure 28**. Ocean temperature (left) and salinity (right) trends for 4 regions (Gulf of Alaska or GOA, central PWS or CS, eastern PWS or E, and the northwestern PWS or NW) for each day of the year (x-axis) and over depth (y-axis). (Figure 3, page 46, Campbell, 2018).

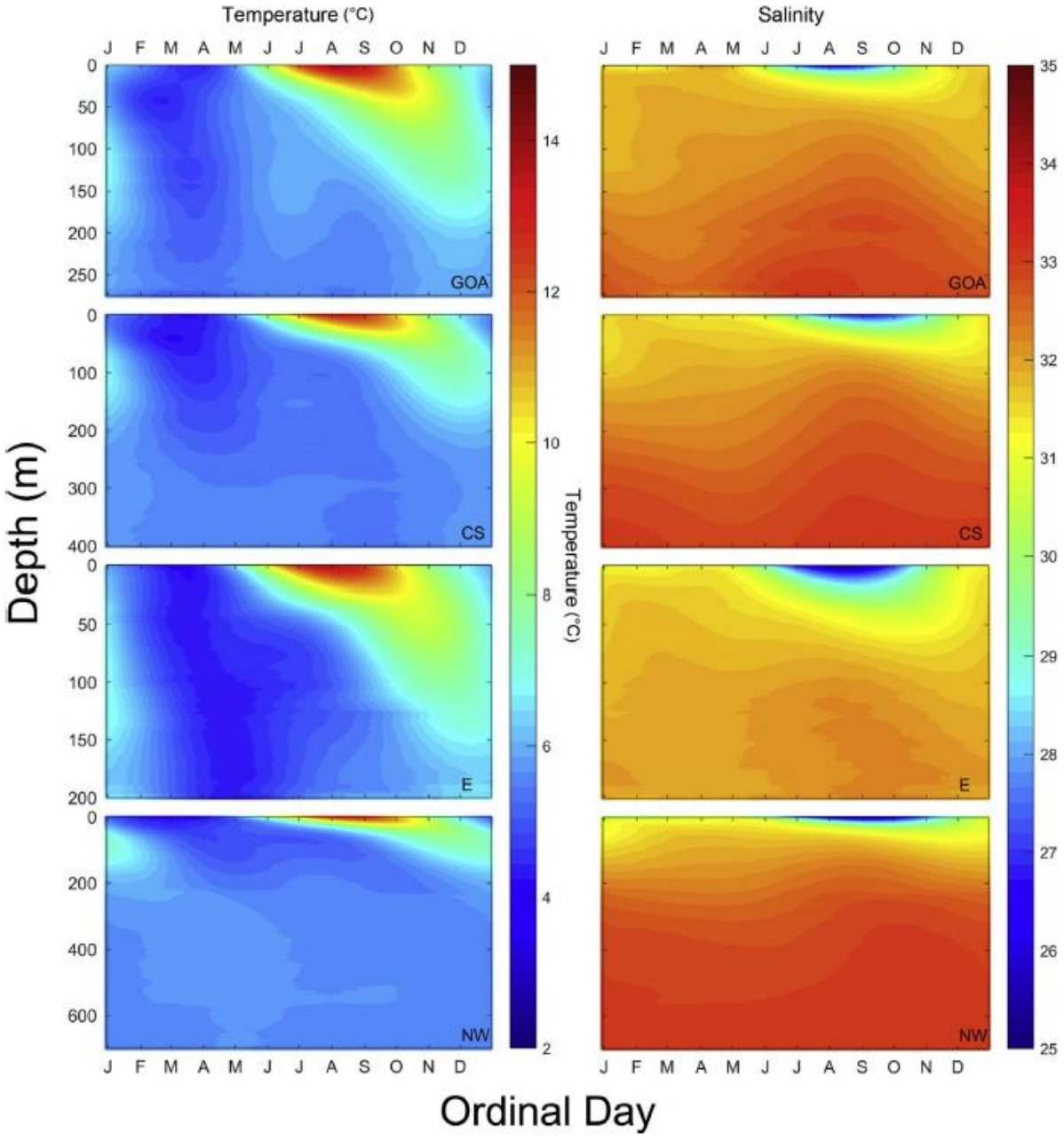

**References Cited:**


Adelfio, L. A. 2016. Geomorphic and climatic controls on water temperature and streambed scour, Copper River Delta, Alaska: Implications for understanding climate change impacts to the Pacific salmon egg incubation environment. M.Sc. thesis, Water Resources Graduate Program, Oregon State University, Corvallis. doi:10.1017/CBO9781107415324.004.

Adelfio, L.A., Wondzell, S.M., Mantua, N.J. and Reeves, G.H., 2018. Warm winters reduce landscape-scale variability in the duration of egg incubation for Coho Salmon (*Oncorhynchus kisutch*) on the Copper River Delta, Alaska. Canadian Journal of Fisheries and Aquatic Sciences https://doi.org/10.1139/cjfas-2018-0152

Alderdice, D.F., and Velsen, F.P.J. 1978. Relation between temperature and incubation time for eggs of Chinook Salmon (*Oncorhynchus tshawytscha*). J. Fish. Res. Board Canada 35(1): 69–75. doi:10.1139/f78-010.

Angilletta Jr, M.J., Ashley Steel, E., Bartz, K.K., Kingsolver, J.G., Scheuerell, M.D., Beckman, B.R. and Crozier, L.G., 2008. Big dams and salmon evolution: changes in thermal regimes and their potential evolutionary consequences. Evolutionary Applications 1: 286-299.

Beacham, T.D., and Murray, C.B. 1990. Temperature, egg size, and development of embryos and alevins of five species of Pacific salmon: A comparative analysis. Trans. Am. Fish. Soc. 119(6): 927–945.

Bieniek, P.A., U.S. Bhatt, R.L. Thoman, H. Angeloff, J. Partain, J. Papineau, F. Fritsch, E. Holloway, J.E. Walsh, C. Daly, M. Shulski, G. Hufford, D.F. Hill, S. Calos, R. Gens. 2012. Climate divisions for Alaska based on objective methods. Journal of Applied Meteorology and Climatology. 51(7): 1276-1289.

Calkin, P.E., G.C. Wiles, and D.J. Barclay. 2001. Holocene coastal glaciation of Alaska. Quat. Sci. Rev. 20:449-461.

Campbell, E.Y., Dunham, J.B., Reeves, G.H. and Wondzell, S.M., 2018. Phenology of hatching, emergence, and end-of-season body size in young-of-year coho salmon in thermally contrasting streams draining the Copper River Delta, Alaska. Canadian Journal of Fisheries and Aquatic Sciences 76: 185-191.

Campbell, R. W. 2018. Hydrographic trends in Prince William Sound, Alaska, 1960–2016. Deep Sea Research Part II, 147: 43-57.

Carlson, S.M. and Seamons, T.R. 2008. A review of quantitative genetic components of fitness in salmonids: implications for adaptation to future change. Evolutionary Applications 1: 222-238.

Cooper, W.S. 1942. Vegetation of the Prince William Sound region, Alaska; With a brief excursion into post-Pleistocene climatic history. Ecological Monographs. 12(1): 1-22.

Crozier, L.G., Hendry, A.P., Lawson, P.W., Quinn, T.P., Mantua, N.J., Battin, J., Shaw, R.G., and Huey, R.B. 2008. Perspective: Potential responses to climate change in organisms with complex life histories: evolution and plasticity in Pacific salmon. Evol. Appl. 1(2): 252–270. doi:10.1111/j.1752-4571.2008.00033.x.

Crozier, L.G. and Zabel, R.W., 2006. Climate impacts at multiple scales: evidence for differential population responses in juvenile Chinook salmon. Journal of Animal Ecology *75*: 1100-1109.

DeVries, P. 1997. Riverine salmonid egg burial depths: review of published data and implications for scour studies. Can. J. Fish. Aquat. Sci. 54(8): 1685-1698. doi:10.1139/f97-090.

Elliott, J.M., Hurley, M.A. and Maberly, S.C., 2000. The emergence period of sea trout fry in a Lake District stream correlates with the North Atlantic Oscillation. *Journal of Fish Biology*, *56*(1), pp.208-210.

Chilcote, M., Coleman, A., Colt, S., Kirchner, P., Reeves, G., Rinella, D., Rothwell, E. and Zemke, S., Salmon. *In* Climate Change Vulnerability Assessment for the Chugach National Forest and the Kenai Peninsula. Gen. Tech. Rep. PNW-GTR-950. *Edited by* G.D. Hayward, S. Colt, M.L. McTeague, and T. Hollingsworth. US Dept. of Agriculture, Forest Service, Pacific Northwest Research Station, Portland, Oregon.

Gay III, S.M. and S.L. Vaughan. 2001. Seasonal hydrography and tidal currents of bays and fjords in Prince William Sound. Fish. Oceanogr. 10(Suppl. 1): 159-193.

Hamlet, A.F. and Lettenmaier, D.P. 2007. Effects of 20th century warming and climate variability on flood risk in the western US. Water Resources Research doi:10.1029/2006WR005099

Hayward, Gregory H.; Colt, Steve; McTeague, Monica L.; Hollingsworth, Teresa N., eds. 2017. Climate change vulnerability assessment for the Chugach National Forest and the Kenai Peninsula. Gen. Tech. Rep. PNW-GTR-950. Portland, OR: U.S. Department of Agriculture, Forest Service, Pacific Northwest Research Station. 340 p.

Helle, J.H. 1970. Biological characteristics of intertidal and fresh-water spawning pink salmon at Olsen Creek, Prince William Sound, Alaska, 1962–63. United States Fish and Wildlife Service, Washington, D.C., Special Scientific Report, Fisheries 602: 19 pp.

Hendry, A.P. and Day, T., 2005. Population structure attributable to reproductive time: isolation by time and adaptation by time. Molecular Ecology 14: 901-916.

Holtby, L.B., 1988. Effects of logging on stream temperatures in Carnation Creek British Columbia, and associated impacts on the coho salmon (*Oncorhynchus kisutch*). Canadian Journal of Fisheries and Aquatic Sciences 45: 502-515.

Holtby, L.B. and Scrivener, J.C., 1989. Observed and simulated effects of climatic variability, clear-cut logging and fishing on the numbers of chum salmon (*Oncorhynchus keta*) and coho salmon (*O. kisutch*) returning to Carnation Creek, British Columbia. Canadian special publication of fisheries and aquatic sciences. 105: 62–81.

Homer, C. G., J. A. Dewitz, L. Yang, S. Jin, P. Danielson, G. Xian, J. Coulston, N. D. Herold, J. D. Wickham, and K. Megown (2015), Completion of the 2011 National Land Cover Database for the conterminous United States-Representing a decade of land cover change information. Photogramm. Eng. Remote Sensing, 81: 345–354.

Isaak, D.J., Luce, C.H., Rieman, B.E., Nagel, D.E., Peterson, E.E., Horan, D.L., Parkes, S. and Chandler, G.L. 2010. Effects of climate change and wildfire on stream temperatures and salmonid thermal habitat in a mountain river network. Ecological Applications 20: 1350-1371.

Kinnison, M.T., Unwin, M.J., Hershberger, W.K. and Quinn, T.P., 1998. Egg size, fecundity, and development rate of two introduced New Zealand chinook salmon (*Oncorhynchus tshawytscha*) populations. Canadian Journal of Fisheries and Aquatic Sciences 55: 1946-1953.

Letcher, B.H., Dubreuil, T., O'Donnell, M.J., Obedzinski, M., Griswold, K. and Nislow, K.H., 2004. Long-term consequences of variation in timing and manner of fry introduction on juvenile Atlantic salmon (*Salmo salar*) growth, survival, and life-history expression. Canadian Journal of Fisheries and Aquatic Sciences 61: 2288-2301.

Mann, D.H. and T.D. Hamilton. 1995. Late Pleistocene and Holocene paleoenvironments of the North Pacific coast. Quat. Sci. Rev. 14:449-471.

Mantua, N., Tohver, I., and Hamlet, A. 2010. Climate change impacts on streamflow extremes and summertime stream temperature and their possible consequences for freshwater salmon habitat in Washington State. Clim. Change 102: 187–223. doi:10.1007/s10584-010-9845-2.

Mantua, N.J., Hare, S.R., Zhang, Y., Wallace, J.M., and Francis, R.C. 1997. A Pacific interdecadal climate oscillation with impacts on salmon production. Bull.

Am. Meteorol. Soc. 78(6): 1069-1079. doi:10.1175/1520-0477(1997)078<1069: APICOW>2.0.CO;2.

McCullough, D.A., 1999. A review and synthesis of effects of alterations to the water temperature regime on freshwater life stages of salmonids, with special reference to Chinook salmon. US Environmental Protection Agency, Region 10. EPA 910-R-99-010

Miller-Rushing, A.J., Høye, T.T., Inouye, D.W. and Post, E., 2010. The effects of phenological mismatches on demography. Philosophical Transactions of the Royal Society B: Biological Sciences 365(1555): 3177-3186.

Mohseni, O., Stefan, H. G., and Erickson, T.R. 1998. A nonlinear regression model for weekly stream temperatures. Water Resour. Res. 34(10): 2685–2692. doi:10.1029/98WR01877.

Neuheimer, A.B. and Taggart, C.T., 2007. The growing degree-day and fish size-at-age: the overlooked metric. Canadian Journal of Fisheries and Aquatic Sciences 64: 375-385.

Neuheimer, A.B. and Taggart, C.T., 2007. The growing degree-day and fish size-at-age: the overlooked metric. Canadian Journal of Fisheries and Aquatic Sciences 64: 375-385.

Schindler, D.E., Rogers, D.E., Scheuerell, M.D. and Abrey, C.A., 2005. Effects of changing climate on zooplankton and juvenile sockeye salmon growth in southwestern Alaska. Ecology 86: 198-209.

Sparks, M.M., Falke, J.A., Quinn, T.P., Adkison, M.D.,Schindler, D.E., Bartz, K.K., Young, D.B., and Westley, P.A.H. 2018. Influences of spawning timing, water temperature, and climatic warming on early life history phenology in western Alaska Sockeye Salmon. Can. J. Fish. Aquat. Sci. doi:10.1139/cjfas-2017-0468.

Tague, C. and Grant, G.E., 2009. Groundwater dynamics mediate low-flow response to global warming in snow-dominated alpine regions. Water Resources Research doi:10.1029/2008WR0071

Thorsteinson, F.V., Helle, J.H. and Birkholz, D.G. 1971. Salmon survival in intertidal zones of Prince William Sound streams in uplifted and subsided areas. In: The Great Alaska earthquake of 1964: biology. National Academy of Science Publication 1604: 194–219.

Wilson, F. H., C. P. Hults, K. A. Labay, and N. Shew (2008), Digital data for the reconnaissance geologic map for Prince William Sound and the Kenai Peninsula, Alaska, *U.S. Geol. Surv. Open-File Rep. 2008-1002*.

van den Berghe, E.P., and Gross, M.R. 1984. Female size and nest depth in coho salmon (*Oncorhynchus kisutch*). Can. J. Fish. Aquat. Sci. 41:204-206. 1139/f84-022.

Zimmerman, C.E., and Finn, J.E. 2012. A simple method for in situ monitoring of water temperature in substrates used by spawning salmonids. J. Fish Wildl. Manage. 3(2): 288-295. doi:10.3996/032012-JFWM-025.

**Table Appendix 1**: Summary list of geologic map units that were combined into a single map group to describe each study watershed, including the Kenai Peninsula, Prince William Sound, and Copper River Delta. Map units follow Wilson et al., 2015.

| Name | Map Unit | Geologic Code | Description |
|---|---|---|---|
| Open Water | 102 | Water | water |
| Perennial Snow and Ice | 101 | Ice | ice |
| Unconsolidated | 100 | Qs | Unconsolidated surficial deposits, undivided (Quaternary) |
| | 105 | Qat | Alluvial and terrace deposits (Quaternary) |
| | 109 | Qat | Alluvial and terrace deposits (Quaternary) |
| | 115 | Qb | Beach deposits (Quaternary) |
| Landslides and Colluvium | 107 | Qls | Landslide and colluvial deposits (Quaternary) |
| | 108 | Qls | Landslide and colluvial deposits (Quaternary) |
| Lacustrine | 112 | Qsl | Lacustrine, swamp, and fine silt deposits (Quaternary) |
| Glacial drift & deposits | 126 | Qm | Glacial deposits (Quaternary) |
| | 130 | Qag | Drift of Neoglacial age (Holocene) |
| Siltstones and siltstone complexes | 680 | Tps | Poul Creek Formation, Sedimentary rocks (Tertiary, early Miocene to late Eocene) |
| | 810 | Tt | Tokun Formation (Tertiary, Eocene) |
| | 820 | Tsw | Stillwater Formation (Tertiary, Eocene) |
| Volcanic | 950 | Tos | Orca Group, Sedimentary rocks, undivided (Tertiary, early middle Eocene to late Paleocene |
| | 951 | Tovs | Volcanic and sedimentary rocks (Tertiary, Eocene) |
| | 2190 | KMm | McHugh Complex (Cretaceous to Mississippian) |
| | 2700 | Kvs | Valdez Group, Metasedimentary rocks, undivided (Upper Cretaceous) |
| | 2702 | ?? | Valdez Group, Interbedded metavolcanic and metasedimentary rocks (Upper Cretaceous) |
| | 2705 | ?? | Valdez Group, Metavolcanic rocks, undivided (Upper Cretaceous) |
| | 2710 | Kvgs | Valdez Group, Schist (Upper Cretaceous) |
| | 1135 | Tov | Volcanic rocks, undivided (Tertiary, Eocene) |
| | 1136 | Top | Pillow basalt (Tertiary, Eocene) |
| Igneous | 1300 | Tgg | Granite and granodiorite (Tertiary, Eocene) |

| | | | |
|---|---|---|---|
| | 1380 | Tmu | Mafic and ultramafic plutonic rocks (Tertiary, Eocene and Paleocene?) |